Detlef Quadfasel
Institut für Meereskunde
Zentrum für Marine und Atmosphärische Wissenschaften
Universität Hamburg
Bundesstr. 53
D-20146 Hamburg

Tel.: +49 40 42838 5756
Fax: +49 40 42838 7477
e-mail: detlef.quadfasel@zmaw.de

Cruise Report
RRS Discovery Cruise D311

Reykjavik - Reykjavik - Reykjavik
8. September – 20.September – 6. October 2006
Chief Scientist: Detlef Quadfasel
Captain: Peter C. Sarjeant

Technical Report 1-06

On citing this report in a bibliography, the reference should be followed by the words *unpublished manuscript.*

The scientific party of RRS DISCOVERY cruise D311 leg 1. The photo was taken after completion of the leg in the port of Reykjavik.

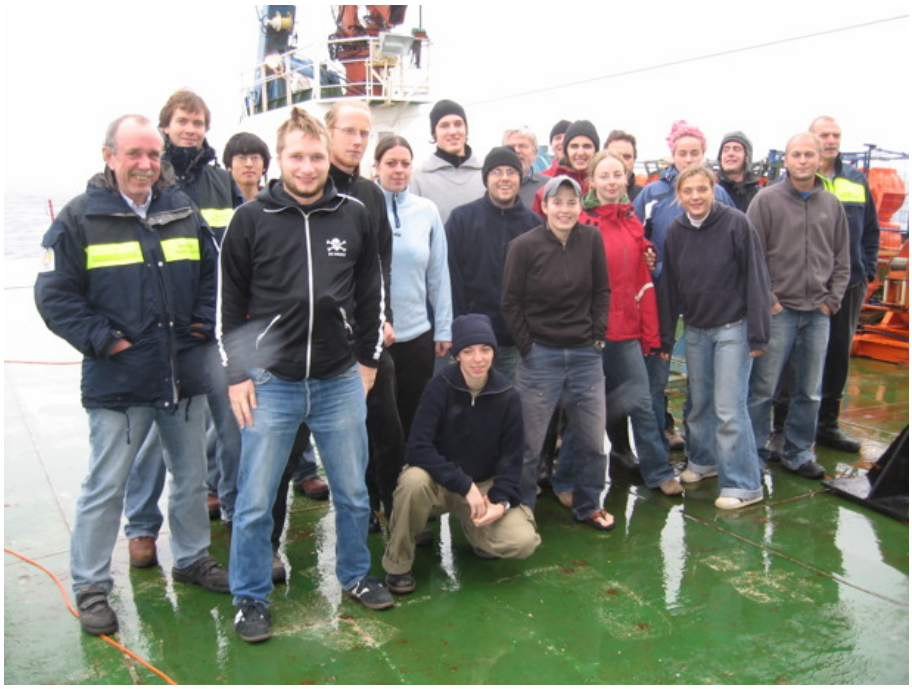

The scientific party of RRS DISCOVERY cruise D311 leg 2. The photo was taken on Discovery's aft deck in wind force 7.

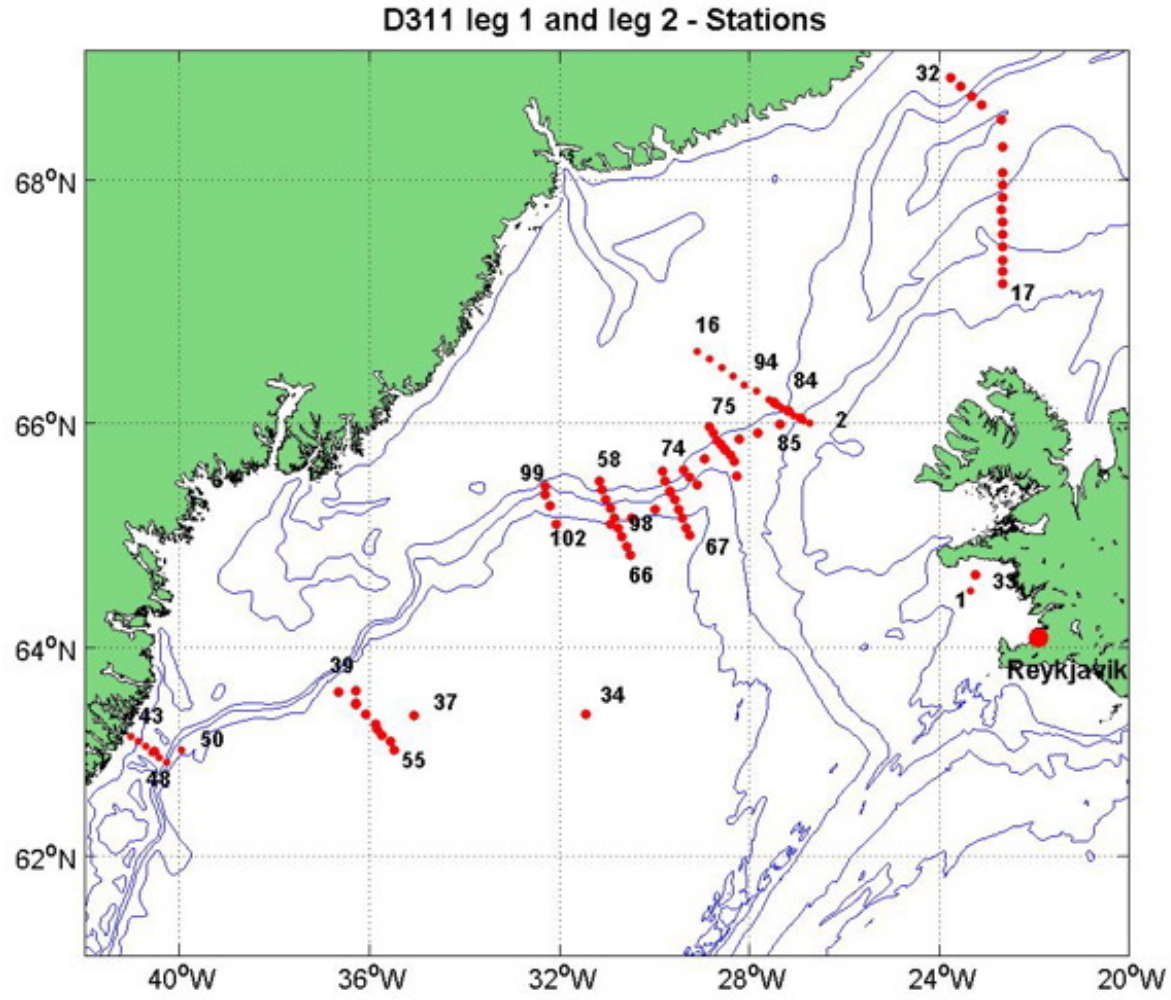

Positions of hydrographic and mooring stations occupied during RRS DISCOVERY cruise D311

1. Objectives

RRS DISCOVERY cruise D311 was carried out by the Institut für Meereskunde at the Centre for Marine and Atmospheric Sciences of the University of Hamburg (IfM-ZMAW), with participation of the Centre for Environment, Fisheries and Aquaculture Science (CEFAS), the Finnish Institute of Marine Research (FIMR), the Woods Hole Oceanographic Institution (WHOI), the Lamont Doherty Earth Observatory (LDEO), the University of Gent (UGent) and the University of East Anglia (UEA).

The objective of Discovery cruise D311 was to study different aspects of the Denmark Strait overflow. The first part of the cruise concentrated on examining the water masses at the sill and the upstream conditions in the East Greenland Current and in the Iceland Sea. Two pathways of overflow water had been discovered north of Denmark Strait. One flows along the Greenland continental slope and involves waters from the Arctic Ocean, Fram Strait and the Greenland Sea. The other runs on the north-western Iceland shelf and apparently carries the densest overflow water. The origin of this water mass is not yet determined. Does it derive from the Iceland Sea or does it come from farther north? To resolve this question the water mass characteristics in the East Greenland Current and in the Iceland Sea was examined by CTD observations and water sampling involving CFCs, H3, He3, O2, O18. In addition attempts to recover moorings were made. The first leg ended in Reykjavik, where exchange of scientific personnel took place.

After the exchange Discovery continued to the Greenland slope, where the VEINS and ASOF CTD sections were taken and the mooring array at Angmassalik recovered and redeployed. The purpose of these sections south of the sill in Denmark Strait is to study the evolution, strength and variability of the overflow plume – how the different water masses from north of the sill mix on their way to the south and how much and by what mechanisms ambient water is entrained into the overflow plume. To study these processes the CTD observations and the water sampling were complemented by turbulence measurements using a freefalling CTD and current meter probe. In addition, an autonomous glider was deployed.

Attending this 4-week cruise, students from the University of Hamburg got the opportunity to practice a scientist's work on board. The students assisted CTD measurements, took water samples and started to process the data obtained. Additionally an oceanographic seminar took place every day. A summary of the students work during the cruise can be found at
http://www.ifm.uni-hamburg.de/~wwwro/quadfasel/teaching/ss2006_discovery/cruise_site/D311_website/index.html

2. Narrative

6. September 2006
Position: Port of Reykjavik

With some delay the containers arrived during the afternoon and were subsequently unloaded. Securing the ROV container on the aft deck required some welding work finished by the early evening.

7. September 2006
Position: Port of Reykjavik

Preparation of the instrumentation continued. All went well, except the tests with the ROV failed. Because of this sailing of the vessel was postponed until noon the next day. The Hamburg students arrived during the afternoon.

8. September 2006
Noon Position: Port of Reykjavik

After breakfast the captain gave a safety briefing for the scientific crew. Several shortcuts in the ROV power supply and data links demanded further repair work. It was decided to postpone sailing to 10 a.m. the next day. During the afternoon the students received an introduction into instrument handling and sampling procedures.

9. September 2006
Noon Position: 64°19.2' N 22°25.6' W
Wind direction: 270° / Wind speed: 20 knots / Air temperature: 9.5°C

After an emergency consultation with the Gent Laboratory it was decided to keep the ROV on board, even though it did not work yet, and to attempt the repair during the cruise. Discovery sailed at 10:00 h. About an hour later the first students became seasick. During the afternoon a CTD test station was run successfully. At 4 p.m. we had an Emergency and lifeboat muster.

10. September 2006
Noon Position: 66°07.2' North / 27°16.2' West
Wind direction: 190° / Wind speed: 18 knots / Air temperature: 7.5°C

Scientific watches started with the morning shift. The CTD section along the sill of Denmark Strait started at 9 a.m. Salinity signals were very noisy and as cleaning of the sensors did not help the pump and conductivity sensor were exchanged. At 1 p.m. an attempt was made to recover the ADCP mooring in Denmark Strait, but no acoustic response was received from the releasers. A release signal was sent anyway, but the mooring did not surface and after an hour we went back to the CTD positions and resumed the hydrographic section.

11. September 2006
Noon Position: 66°10.6' North / 27°29.0' West
Wind direction: 210° / Wind speed: 20 knots / Air temperature: 3.3°C

On station 6 the pump of the CTD broke and had to be replaced. The sensor package was moved from the fin to the interior of the rosette, which reduced the noise on the traces significantly. During the day the weather improved and the Denmark Strait section was continued. A first sighting of whales caused excitement with the students. During the night colourful northern lights showed up at the horizon.

12. September 2006
Noon Position: 66°52.0' North / 26°47.1' West
Wind direction: 070° / Wind speed: 18 knots / Air temperature: 3.3°C

After 16 stations the Denmark Strait section was completed at 9 a.m. Because of a gale warning we decided to steam north to run a CTD section along 21° 40' W, from the shelf break of Iceland to the north. In the evening we had a little party celebrating the crossing of the Arctic Circle the night before. The first station (No. 17) of the second section was reached at 9 p.m.

13. September 2006
Noon Position: 67°32.4' North / 22°26.2' West
Wind direction: 070° / Wind speed: 40 knots / Air temperature: 5.3°C

Increasing winds forced us to stop work at station 19 and the ship had to stay hove to.

The students started with working up the CTD data and were assigned small scientific projects.

14. September 2006
Noon Postion: 67°26.8' North / 22°45.9' West
Wind direction: 055° / Wind speed: 35-40 knots / Air temperature: 5.0°C

The weather did not improve and the ship stayed hove to. The captain started a series of navigation courses for the students, which was extremely well received.

15. September 2006
Noon Position: 67°39.5' North / 22°27.6' West
Wind direction: 045° / Wind speed: 40 knots / Air temperature: 2.6°C

No change of weather. The day was spent with student seminars and a test of their knowledge on security procedures. Because of cheating Koen was disqualified; Alison won by scoring 21 points. Her prize was a Discovery mug.

16. September 2006
Noon Position: 67°51.7' North / 22°14. 5' West
Wind direction: 020° / Wind speed: 20-25 knots / Air temperature: 2.8°C

The weather improved slightly and by 10:30 a.m. we sailed back to position 20 on the CTD section. Work resumed at 3 p.m.

17. September 2006
Noon Position: 68°35.8' North / 22°06.4' West
Wind direction: 045° / Wind speed: 25 knots / Air temperature: 0.6°C

During the night winds were very calm and good progress was made along the section. However, since the forecast was bad again, some stations were skipped in order to complete the section across the East Greenland continental slope The weather became worse again in the afternoon but we were able to work until 9 p.m. by which time wind reached 9 Bft. The students enjoyed a beautiful sunset over the Greenland glaciers before they had a theory lesson given by Professor Zahel. Due to the strong winds and swell from the north-east it was decided to change the mid-cruise port call from Akureyri to Reykjavik and the agent and scientists for the next leg were informed accordingly.

18. September 2006
Noon Position: 66°31.4' North / 25°16.3' West
Wind direction: 055° / Wind speed: 45 knots / Air temperature: 3.6°C

Steaming towards Reykjavik with 10m swell from aft. This was an impressive roller coaster ride under a blue sky. The students were busy working up data preparing the project presentations. In the evening the Belgian colleagues gave a presentation about their ROV, which by then worked properly, at least in the hangar.

19. September 2006
Noon Position: 64°40.0' North / 23°13.7' West
Wind direction: 070° / Wind speed: 18 knots / Air temperature: 11.8°C

We were once again near the Icelandic coast with a beautiful view over and in shelter of snow covered mountains. Jules Verne used one of those volcanoes as an entrance to his travel to the middle of the earth. The ROV was launched in a water depth of 70 m and provided pictures of the shelf bottom. The instrument worked well – finally – but unfortunately too late for the planned mooring recovery work. Discovery went alongside

in Reykjavik harbour at 8 p.m. and the first leg of cruise D311 was finished. The evening saw the student's project presentations, which were followed by a little farewell party.

20. September 2006
Noon position: Port of Reykjavik

The new scientific crew arrived at 10 a.m. and the "old" student-crew left at 1 p.m. for the airport. The ROV container was offloaded and the equipment for the microstructure probe was taken on board. Discovery sailed at 3 p.m., heading for the line of moorings to be recovered and re-deployed.

21. September 2006
Noon position: 63°44.6' North / 30°03.2' West
Wind direction: 045° / Wind speed: 20 knots / Air temperature: 8.4°C

At 4 p.m. a test of the Microstructure probe was attempted, but before going into the water some problems occurred with the winch system and the test was abandoned.

22. September 2006
Noon position: 63°20.2' North / 36°00.1' West
Wind direction: various / Wind speed: light airs / Air temperature: 7.5°C

Discovery reached the first mooring position at 6 a.m. but the release of the mooring failed. No response signal was detected. After several tries it was decided to move to the next mooring and by 6 p.m. all four remaining moorings along the Angmassalik line were recovered. We then sailed to the position of the shallow moorings on the East Greenland shelf.

23. September 2006
Noon position: 63°00.3' North / 40°33.2' West
Wind direction: 025° / Wind speed: 25 knots / Air temperature: 1.4°C

The bottom mounted ADCP mooring was successfully grappled at 9:30 a.m. and was on deck half an hour later. After an unsuccessful attempt to recover tube-mooring 21 we deployed its replacement by 4.30 p.m. A CTD section was then run across the shelf with the first station being only 3 miles off the Greenland coast. Unfortunately the weather was quite foggy so the tourist aspects of this section were not met too well. The section was then run offshore, out of the region where many icebergs were floating around.

24. September 2006
Noon position: 63° 01.1' North / 40° 34.5' West
Wind direction: 015° / Wind speed: 45-55 knots / Air temperature: 1.8°C

During the night the weather became increasingly stormy, so we had to stop our work after station 48 was completed at 4 a.m.. Discovery stayed hove to throughout the day and the time was spent with data analysis and student seminars.

25. September 2006
Noon position: 63° 01.1' North / 40° 29.3' West
Wind direction: 030° / Wind speed: 30 knots / Air temperature: 4.6°C

Winds ceased slightly during the night and we were able to reach the ADCP deployment position by 8:30 a.m. The ADCP with a ground line was successfully deployed by noon. After one more CTD station the WHOI glider was deployed during the afternoon and we steamed back to the Angmassalik array location.

26. September 2006
Noon position: 63° 30.8' North / 36° 24.9' West
Wind direction: 070° / Wind speed: 20 knots / Air temperature: 9.3°C

Except for the dense fog the weather conditions were perfect for the mooring deployments, which started at 9 a.m. with mooring F1/2 and finished with the fourth mooring UK2 at 6 p.m. Because of the fog no attempt was made to recover the Aqualab, but instead another Microstructure probe trial was made. Again there were problems with the winch and the test had to be abandoned. A second attempt to make contact with mooring G2 failed and a CTD section along the mooring line was started.

27. September 2006
Noon position: 63° 14.1' North / 35° 51.2' West
Wind direction: 040° / Wind speed: 30 knots / Air temperature: 8.4°C

Stephen Dye's birthday. With winds gusting to 45 knots work had to be abandoned by 1 a.m. Two more CTD profiles were taken during the morning, when winds appeared to calm down, but by noon winds and waves had picked up again so that no more work was possible. Discovery sailed to the Aqualab position where acoustic contact was made, but due to the heavy swell we decided against releasing the mooring. Since the weather forecast for the region showed winds of 8 Bft. for the next two days, we decided to sail north towards Denmark Strait.

28. September 2006
Noon position: 63° 59.5' North / 34° 11.6' West
Wind direction: 045° / Wind speed: 50 knots / Air temperature: 5.3°C

It was stormy the whole day with wave heights of up to 9 meters. The ship's speed was just about 2 knots. The students spent the day in front of the computers, and were given a course in knot making by the bosun. Also the captain gave a course in navigation. In groups of three students were allowed to go up and ask everything about the instruments on the bridge. Stephen Dye gave a presentation on 'Overflow and freshwater: Ocean fluxes south of Denmark Strait'.

29. September 2006
Noon position: 64° 59.5' North / 31° 53.3' West
Wind direction: 030° / Wind speed: 35 knots / Air temperature: 4.8°C

During the day the swell ceased slightly allowing another test of the Microstructure probe. For the first time the instrument worked properly. During the night we continued with a CTD section across the overflow plume

30. September 2006
Noon position: 64°55.1' North / 30°35.3' West
Wind direction: 025°/ Wind speed: 18 knots / Air temperature: 5.6°C

The weather was good and the mood of the scientists was the same: the sun was shining, the sea was calm and we saw a lot of whales again. A pod of more than ten Pilot whales swam right beside the ship, spouting water. In the afternoon we discontinued the current CTD section because it had passed the overflow plume. We started a new section some 30 miles upstream, had a great sunset and fantastic northern lights later in the night. Unfortunately the slip rings in the Microstructure winch had been flooded with sea water and required some cleaning and repair.

1. October 2006
Noon position: 65° 46.0' North / 29° 20.0' West
Wind direction: various / Wind speed: light airs / Air temperature: 4.4°C

Perfect weather again. The CTD and Microstructure work went smoothly and it was decided to drag for the mooring in Denmark Strait the next day, after finishing the hydrographic sections in the south.

2. October 2006
Noon position: 66° 07.2' North / 27° 16.5' West
Wind direction: 160° / Wind speed: 12 knots / Air temperature: 4.1°C

The final CTD station on the section ended at 5 a.m. and by 9 a.m. Discovery reached the mooring position on the Denmark Strait sill. Two attempts were made with 1600 m of wire out, but both of them were not successful. (It turned out later, that the mooring had broken off the anchor about 3 weeks earlier. It was found drifting and recovered by Faroese fishermen who delivered it back to the Faroese Oceanographic Institute). After lunch the students had the opportunity to visit the engine room. At 6 p.m. CTD work was taken up again.

3. October 2006
Noon position: 65°31.5' North / 29°15.7' West
Wind direction: 190° / Wind speed: 17 knots / Air temperature: 7.8°C

CTD work continued throughout the day, after completing the Denmark Strait section we ran another one along the bottom topography following the overflow plume downstream.

4. October 2006
Noon position: 65°16.9' North / 32°12.1' West
Wind direction: 010° / Wind speed: 20 knots / Air temperature: 3.9°C

We completed our last CTD measurement at 4 p.m. and Discovery set course to Reykjavik Harbour. Instrumentation was stored away, laboratories cleaned and the evening saw a great party, organized by Bert Rudels on the occasion of his birthday. We also held a photo competition that was won by Alison with her picture of a big wave.

5. October 2006
Noon position: 64°58.8' North / 32°12.1' West
Wind direction: 070° / Wind speed: 15 knots / Air temperature: 8.0°C

Continued cleaning and packing. Discovery was alongside at 8 p.m. and cruise D311 ended.

6. October 2006
Noon position: Reykjavik Harbour

Demobilising, packing of the containers ashore. The scientific party disembarked at around noon.

3. Cruise participants

Scientific party:

Participants leg 1:

Detlef Quadfasel (Ch.Sc.)	IfM – ZMAW	detlef.quadfasel(at)zmaw.de
Andreas Welsch	IfM – ZMAW	andreas.welsch(at)zmaw.de
Norbert Verch	IfM – ZMAW	norbert.verch(at)zmaw.de
Wilfried Zahel	IfM – ZMAW	wilfried.zahel(at)zmaw.de
Bert Rudels	FIMR	rudels(at)fimr.fi
Alison Criscitiello	LDEO	crisciti(at)ldeo.columbia.edu
Willem Versteeg	UGent	willem.versteeg(at)ugent.be
Jeroen Vercruysse	UGent	jeroenvercruysse(at)telenet.be
Koen De Rycker	UGent	koen.derycker(at)ugent.be

Meike Kühnel	student IfM
Gerrit Maschwitz	student IfM
Antje Müller-Michaelis	student IfM
Katharina Prenzel	student IfM
Nicole Rüther	student IfM
Anna Catrin Schmidt	student IfM
Anna Sellhorn Timm	student IfM
Rita Thönnes	student IfM
Moritz Wellner	student IfM
Max Wicklein	student IfM

Participants leg 2:

Detlef Quadfasel (Ch.Sc.)	IfM – ZMAW	detlef.quadfasel(at)zmaw.de
Andreas Welsch	IfM – ZMAW	andreas.welsch(at)zmaw.de
Norbert Verch	IfM – ZMAW	norbert(at)zmaw.de
Gunnar Voet	IfM – ZMAW	gunnar.voet(at)zmaw.de
Bert Rudels	FIMR	rudels(at)fimar.fi
Stephen Dye	CEFAS	s.r.dye(at)cefas.co.uk
Neil Needham	CEFAS	neil.needham(at)cefas.co.uk
Peter Winsor	WHOI	pwinsor(at)whoi.edu
Peter Sugimura	WHOI	psugimura(at)whoi.edu
Alison Criscitiello	LDEO	crisciti(at)ldeo.columbia.edu
Gareth Alan Lee	UEA	G.A.Lee(at)uea.ac.uk

Antje Müller-Michaelis	student IfM
Alexander Beitsch	student IfM
Simon Brinkrolf	student IfM
Nina Maaß	student IfM
Michaela Markovic	student IfM
Lucia Rau	student IfM
Theresa Reichelt	student IfM
Bente Tiedje	student IfM
Christian Zoller	student IfM

IfM-ZMAW: Institut für Meereskunde
Centre for Marine and Atmospheric Sciences
University of Hamburg
Bundesstr. 53
D-22529 Hamburg
Germany

CEFAS: Centre for Environment, Fishery and Aquaculture Sciences
Lowestoft Laboratory
Pakefield Road
Lowestoft Suffolk NR33 0HT
U.K.

UEA: School of Environmental Sciences
University of East Anglia
Norwich NR4 7TJ
U.K.

FIMR: Finnish Institute of Marine Research
P.O. Box 33
FIN-00931 Helsinki
Finland

WHOI: Woods Hole Oceanographic Institution
266 Woods Hole Road
Woods Hole, MA 02543-1050
U.S.A.

UGent: Renard Centre of Marine Geology
Department of Geology and Soil Science
Ghent University
Krijgslaan 281 s.8
B-9000 Gent
Belgium

LDEO: Lamont Doherty Earth Observatory
PO Box 1000
Palisades, NY 10964-8000
U.S.A.

UKORS technical staff:

Martin Bridger	TECH	UKORS
Darren Young	TECH	UKORS
John Wynar	TECH	UKORS

UKORS: Ocean Engineering Division
United Kingdom Ocean Research Services
Southampton Oceanographic Centre
European Way
Southampton SO14 3ZH
U.K.

Ship crew:

Peter C. Sarjeant	MASTER
Philip D. Gauld	C/O
Annalara P. Kirkaldi-Willis	2/O
Katie E. Rumbold	3/O
David S. Bendell	Cadet
Stephen A. Moss	C/E
Stephen J. Bell	2/E
Gary Slater	3/E
Anthony Healy	3/E
Dennis WJ Jakobaufderstroth	ETO
David R. Hartshorne	PCO
Michael J Drayton	CPOD
Michael Minnock	CPOS
Philip Allison	Seaman
Gerald Cooper	SG1A
Gary Crabb	SG1A
William M McGeown	Sm/Grade
Lee Stephens	S/Man 1A
Leslie J Hillier	MM1A
John Haughton	Chef
Stephen R Nagle	Chef
Darren A Caines	Asst Chef
Graham M Mingay	Stwd

5. Technical information

John Wynar

CTD system

A total of 88 CTD casts were completed on this cruise, the numbering of each cast being some-what unconventional. Each site occupied had a separate station number, and if a CTD was repeated it's cast number was incremented. The initial sensor configuration was as follows:

Sea-Bird 9*plus* underwater unit, s/n 09P-37898-0782
Sea-Bird 3 Premium temperature sensor, s/n 03P-4489 (Frequency 0)
Sea-Bird 4 conductivity sensor, s/n 04C-2407 (Frequency 1)
Digiquartz temperature compensated pressure sensor, s/n 94756 (Frequency 2)
Sea-Bird 3 Premium temperature sensor, s/n 03P-4490 (Frequency 3)
Sea-Bird 4 conductivity sensor, s/n 04C-2450 (Frequency 4)
Sea-Bird 43 dissolved oxygen sensor, s/n 43-0612 (V0)
Benthos PSA-916T 7Hz altimeter, s/n 1040 (V2)
Chelsea Aquatracka MKIII fluorometer, s/n 88-2360-108 (V3)
WETLabs Light Scattering sensor, s/n BBRTD-169 (V6)
Chelsea Alphatracka MKII transmissometer, s/n 04-4223-001 (V7)
Sea-Bird 11*plus* deck unit, s/n 11P-19817-0495

Ancillary instruments & components:

Sea-Bird 24-position Carousel, s/n 32-24680-0344
NOC/SBE 'Break-Out Box', s/n BO19107T
NOC 10KHz acoustic pinger, s/n B12
Sonardyne HF Deep Marker Beacon, s/n 215303-01
RDI WorkHorse Monitor 300KHz ADCP, s/n 1881 (Master: downward-looking)
RDI WorkHorse Monitor 300KHz ADCP, s/n 5414 (Slave: upward-looking)
NOC/RDI aluminium Workhorse battery pack, s/n WH001
14 x Ocean Test Equipment ES-10L water samplers, s/n 01 to 14 inc.

User supplied instrument:

SBE35RT temperature sensor, s/n: 43585-0028

CTD analysis & changes to configuration:

A) Prior to the station/cast 1/1, the Break-Out Box or BOB (s/n: BO19106) was replaced due to severe corrosion across the power and ground pins of the JT5/Aux3 bulkhead connector. It was exchanged with the titanium BOB (s/n: BO19107T).

B) Data spikes on the primary salinity display were observed on the first "shake-down" station 1/1, and the 11*plus* deck unit indicated that the primary pump was not operating occasionally on the downcast. Connectors on the instruments and the cables were cleaned and inspected, but the fault repeated and even deteriorated during the next cast, 2/1. The primary conductivity cell (s/n: 4C-2407) and it's cable was replaced (with s/n: 4C-2164) resulting in considerably fewer data spikes on the next cast, 2/a. The pump also operated normally for both the downcast and upcast. To attempt to remove the remaining data spikes, the primary temperature sensor (s/n: 3P-4489) was replaced (with s/n: 3P-4151). The following station, 3/1 produced fewer data spikes still, and all subsequent ones showed no further spikes.

C) During station 3/1 the altimeter display remained at 0 for the entire cast. Removing and cleaning connectors had no effect so the altimeter (s/n: 1040) was replaced with the spare Benthos unit (s/n: 1037). This again made no difference until the altimeter was re-selected in the Seasave software. It then began to display the correct in-air value of 98.5. It was speculated that the fault lay in the software and not hardware and that the altimeters would be exchanged at some convenient time to prove this. This happened prior to station 20/1 when the original Benthos altimeter was fitted. The altimeter display operated normally, hence the original unit (s/n: 1040) was left in place.

D) CTD cast 6/1 was abandoned due to a re-occurrence of severe data spiking. The replay indicated that the spiking began on the secondary channel before it affected the primary. Examination of the instrument revealed a broken connector on the secondary pump (s/n: 053965). The secondary instruments had been fitted to the CTD vane on a previous cruise, with the pump attached on the vane and slightly proud of it, nearest to the frame and close to a vertical frame member. This left the pump connector vulnerable to any lateral movement of the vane relative to the frame. Hence, the damage was most likely caused by the vane striking the ship's side during deployment, the vane flexing forcing the pump connector against the CTD frame's vertical member and breaking it. Subsequent dismantling of the pump showed it had flooded, the resultant short-circuiting of power and data lines producing the data spikes. The pump was replaced (by s/n: 054164) and the secondary instruments re-positioned inside the frame, conventionally fitted to the SBE 9+ fish.

E) Data spikes on the BBRTD channel had been getting progressively worse. Cleaning the connectors had some limited effect but did not eliminate the problem. The lead from the BBRTD to the BOB was replaced and cured the fault. Close inspection of the BOB connector of the cable indicated some water ingress causing the data loss.

F) The RDI WorkHorse Monitor ADCP's performed as expected for the duration of the cruise, with the exception of no Slave data in the following files:

D311_27s
D311_31s
D311_60s
D311_63s
D311_67s
D311_90s
D311_98s

Examination of the log file revealed no errors in the command file sent to the instrument, nor were there any errors or data problems with the corresponding Master data. Command files used throughout the cruise are attached. The exception was D311_063 where the communications lead was inadvertently disconnected before the command file was transmitted.
Note that LADCP data was only collected for CTD casts deeper than approximately 700m, the nominal range of the Ocean Surveyor 75kHz ship-fitted ADCP.

G) Copies of the Sea-Bird SeaSave configuration files are attached, one for the initial .CON file, one for the conductivity cell replacement .CON file, and one for the temperature sensor replacement. A separate .CON file is not included here (for the sake of brevity) when the altimeter was changed as it did not involve any change in coefficients.

Other instruments

1) Guildline Autosal 8400B salinometer, s/n: 60839. A total of 441 salinity samples were taken during the cruise for CTD analysis. The salinometer was sited in the Constant Temperature Lab, with the bath temperature set at 21C, 1 to 2 degrees above ambient temperature. Softsal was used as the data recording program for salinity values, and results were plotted via an Excel spreadsheet. Stn/cast 3/1, bottle 3 shows an anomalously low primary salinity value compared with the autosal and the secondary salinity channel. This was due to a data spike occurring at the exact moment of bottle firing as replaying the cast revealed. Stn/cast 67/1 shows a discrepancy between the Autosal salinity measurement and the values given by the CTD. This is probably due to contamination of the sample taken in marginal conditions.

6. Student projects - preliminary results

Sea surface temperature and salinities in Denmark Strait

Between Iceland and Greenland, in Denmark-Strait two water masses meet; Polar Water from the Arctic Ocean and the Atlantic Water from the south.

To study the distribution of water masses and their mixing we sampled near surface salinity and temperature data with a thermosalinograph (TSG) every 30 seconds. The TSG was calibrated with CTD-Data and water samples drawn at the instrument's intake. The offset of the TSG is 0.144 for salinity and 0.04 for temperature. After some editing the data were averaged over 10 minute intervals.

In the TS-Diagram the two water masses can be clearly identified, the warm and saline Atlantic water and a nearly straight line of cold and fresh Polar water. Most of the data points are scattered around 3° C and 32.5 and indicate mixing between the Polar and Atlantic Waters.

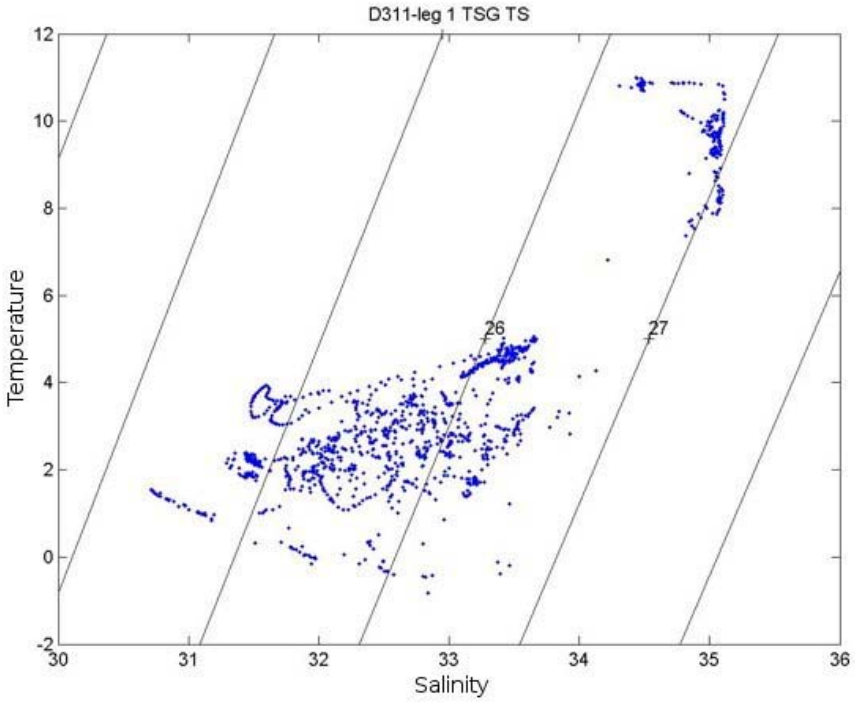

Figure 1: TS-Diagram from TSG-Data

The regional distribution of salinity and temperature shows the warm and saline Atlantic Water west and north of Iceland. It is carried by the Irminger-Current flowing from the south into the Nordic Seas. The cold and low salinity, down to 31 psu, water found at the continental slope of east Greenland, indicates the presence of Polar Water. It flows southward in the East-Greenland-Current.

Some low salinity water appears to turn eastward near 68°N and may be associated with the North Icelandic Current. In Denmark Strait the front between Polar and Atlantic Water is very sharp, while in the north the weaker gradients indicate mixing between the two water masses, possibly associated with meso-scale eddy activity.

West of the path of Polar Water, on the east Greenland shelf, surface salinities are again as high as 33.5, indicating a strong contribution of Atlantic Water. Recirculation of the Irminger-Current, a second separate current from the Atlantic or an eddy are possible scenarios. For an accurate identification we would need more measurements, such as CTD and current profiles.

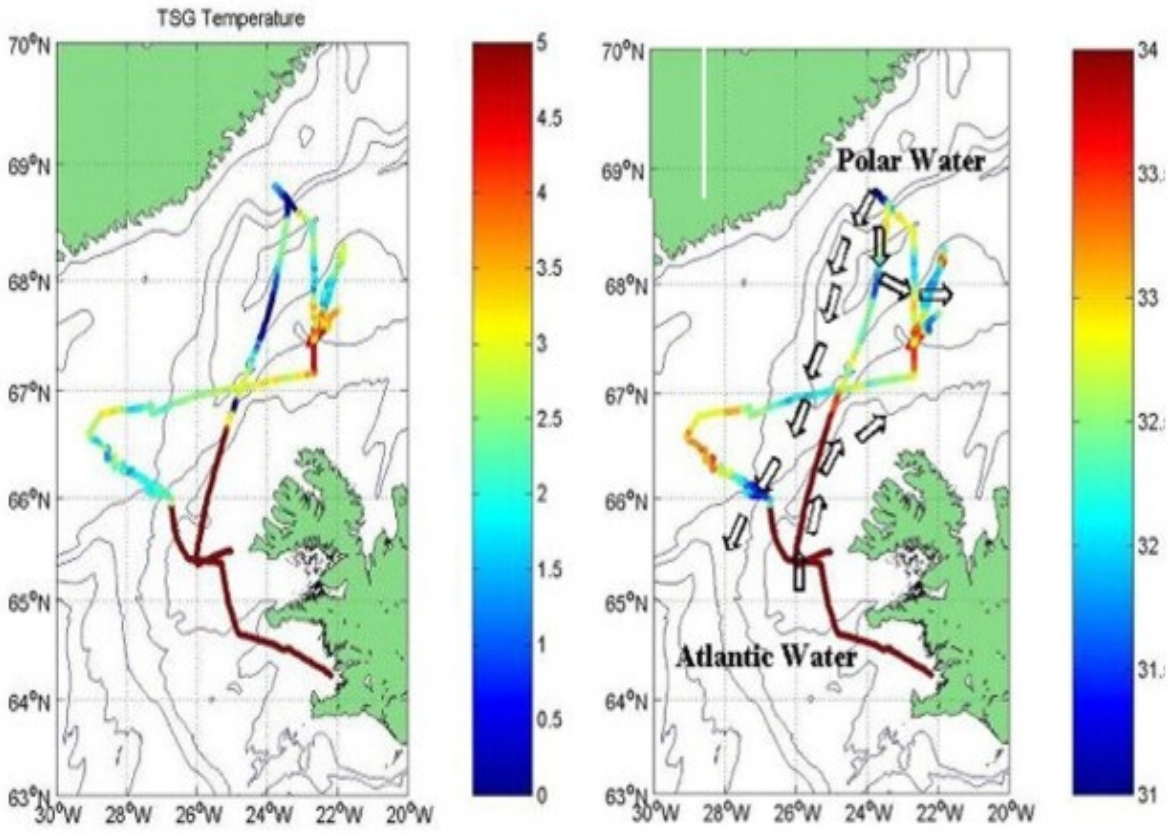

Figures 1 / 2: The mean (every 20 data) Temperature / Salinity after cleaning the output data

Sources of the Denmark Strait Overflow

An aim of the cruise D311 with the Research Vessel Discovery to the Denmark Strait was to determine the sources of the Denmark Strait Overflow Water. Here we present a preliminary attempt to determine these sources using the data from two sections, one along the sill and one north of the Denmark Strait. Because of the adverse weather condition no stations were taken in the Iceland Sea and here we use data from profiling Argo floats deployed in October 2005.

The Overflow comprises dense waters from the Nordic Seas and the Arctic Ocean that cross the Greenland- Scotland- Ridge and sink into the deep North Atlantic, contributing to the NADW. To sink into the deep North Atlantic the water crossing the 600m sill in the Denmark Strait must be denser than 27.8. TS-curves (Figure 4) and potential temperature and salinity sections taken at the sill (Figures 5, 6) show that the overflow temperature ranges from -0.3°C to above 2°C and the salinity lies between 34.8-34.92.

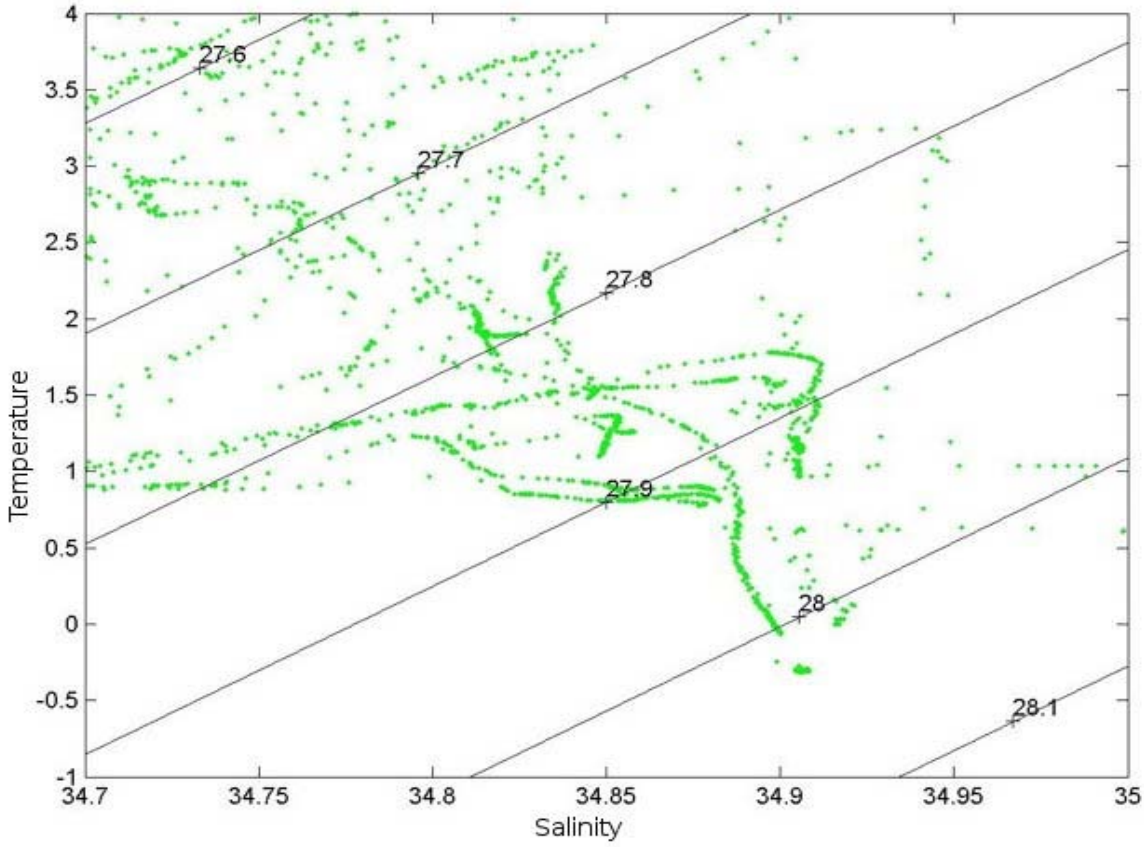

Figure 4: TS-diagram section 1 (sill of the Denmark Strait)

There are two principal hypotheses concerning its sources.

1) The origin of the Denmark Strait Overflow water (DSOW) is the East Greenland Current (EGC), which carries dense Arctic Atlantic Water and intermediate water from the Arctic Ocean. Recirculating warm but dense Atlantic Water from Fram Strait as well as colder dense Arctic Intermediate Water from Greenland Sea.
2) The main source is the intermediate water formed in the Iceland Sea, which then would provide the densest part of the overflow.

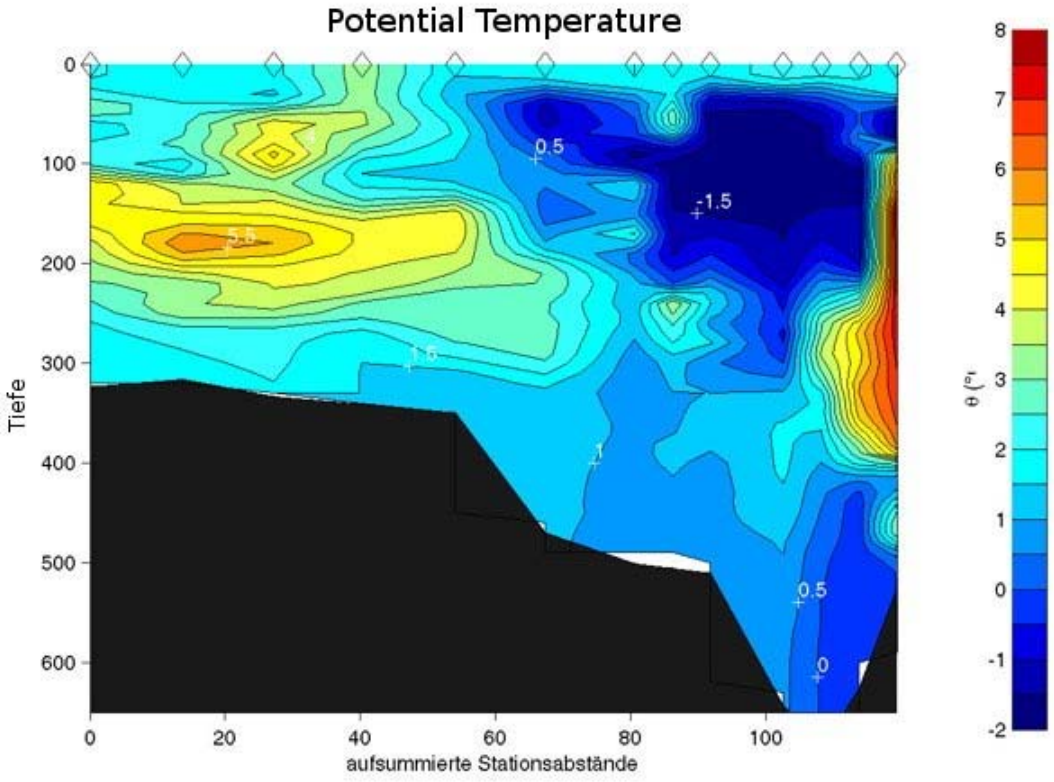

Figure 5: Distribution of Potential Temperature, section 1 (Denmark Strait)

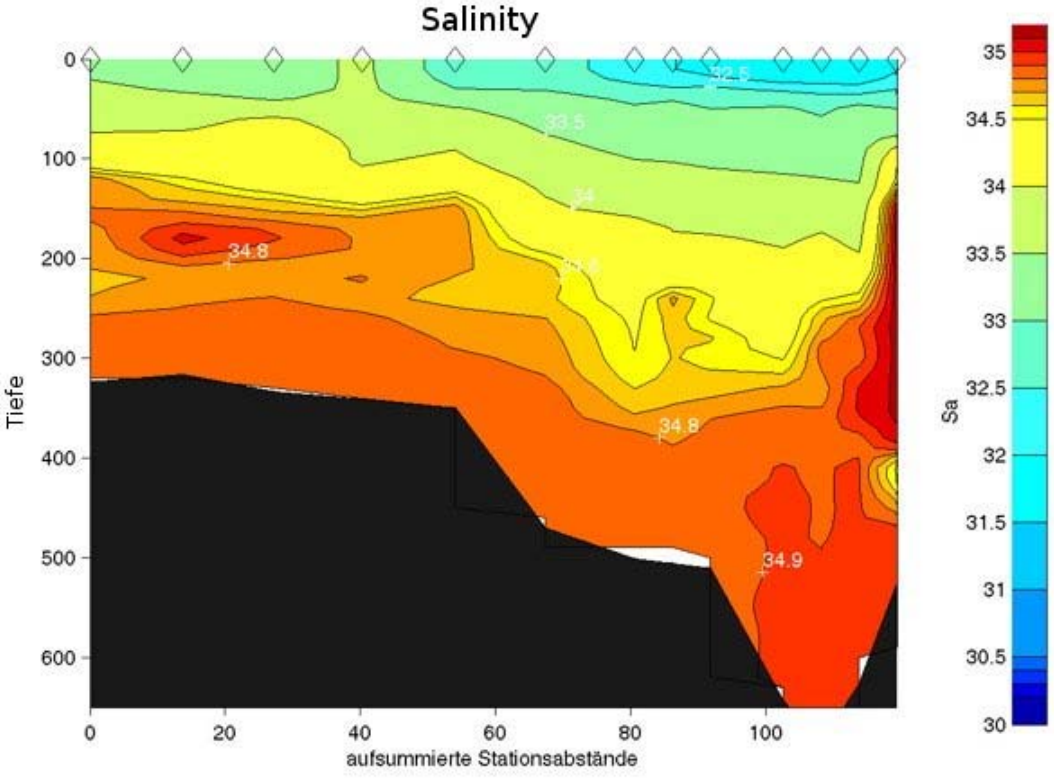

Figure 6: Distribution of Salinity, section 1 (Denmark Strait)

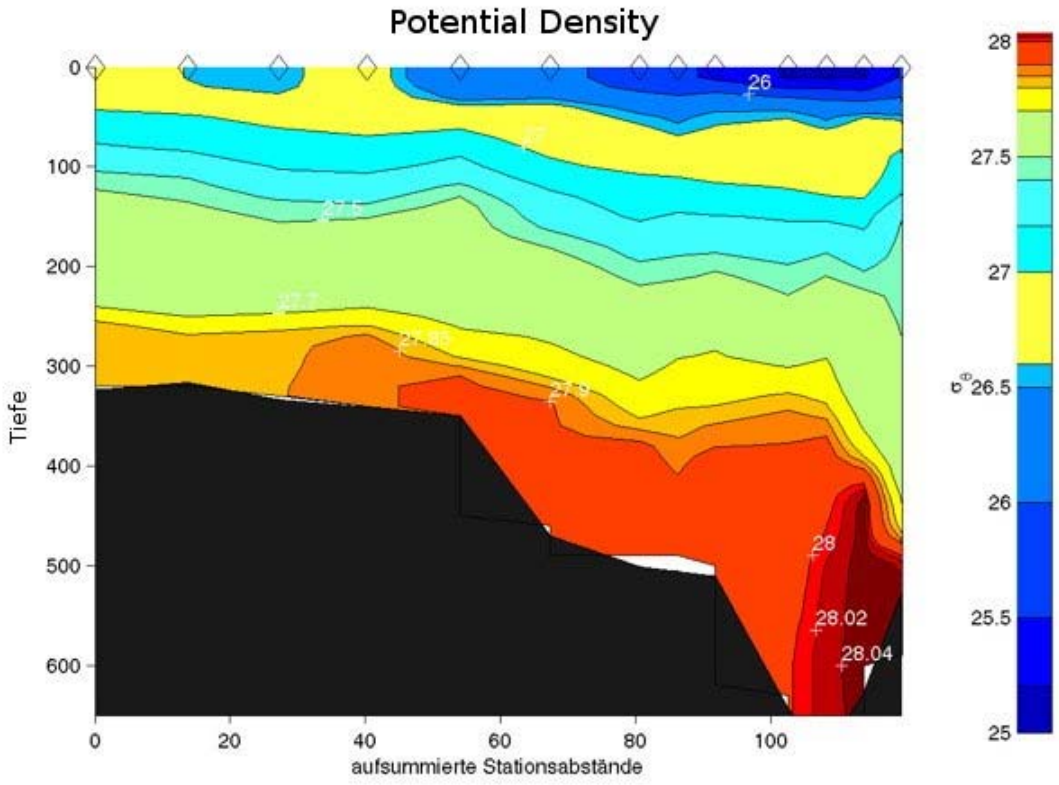

Figure 7: Distribution of Potential Density, section 1 (Denmark Strait)

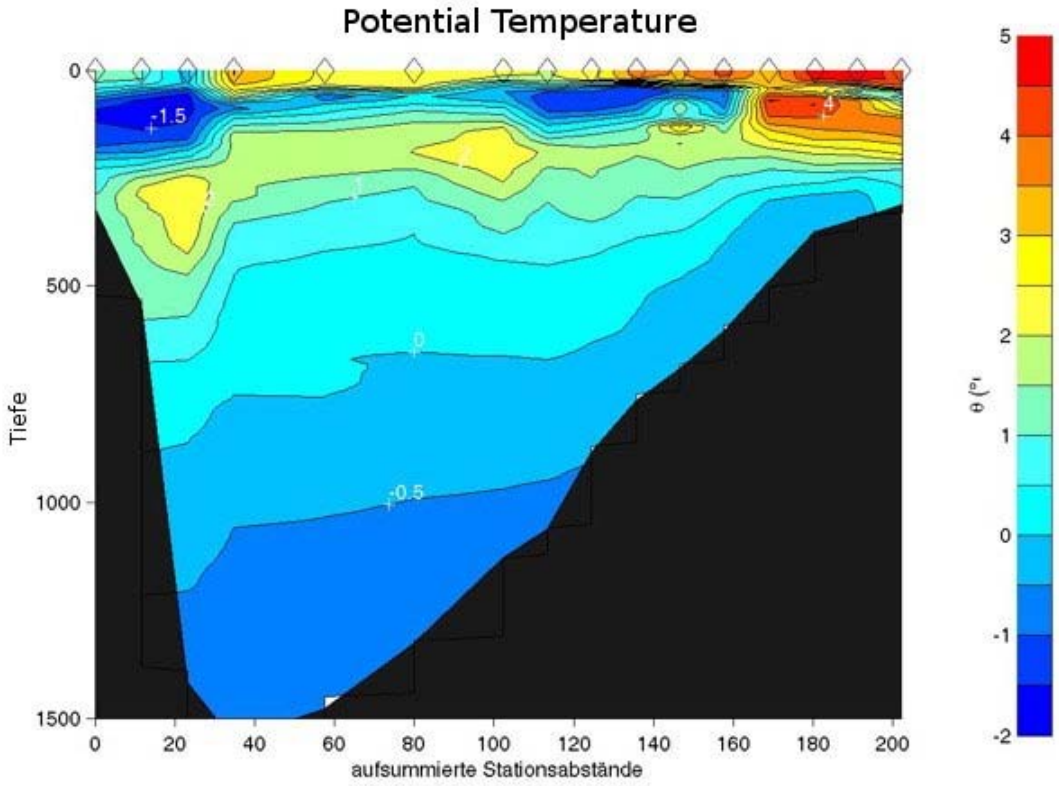

Figure 8: Distribution of Potential Temperature, section 2 (north of Denmark Strait)

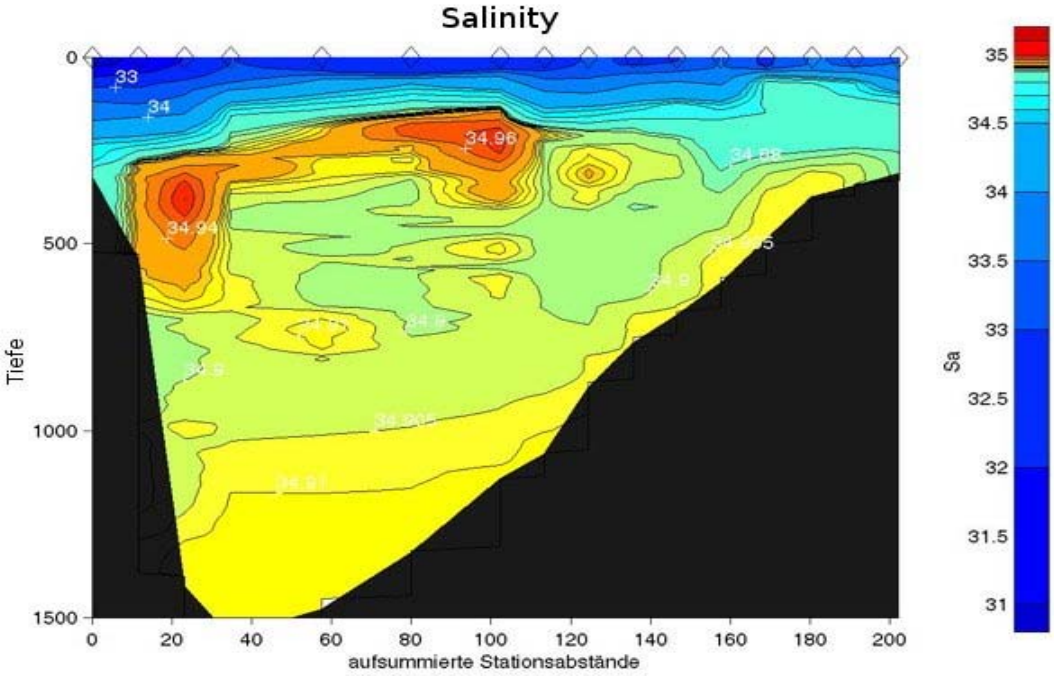

Figure 9: Distribution of Salinity, section 2 (north of Denmark Strait)

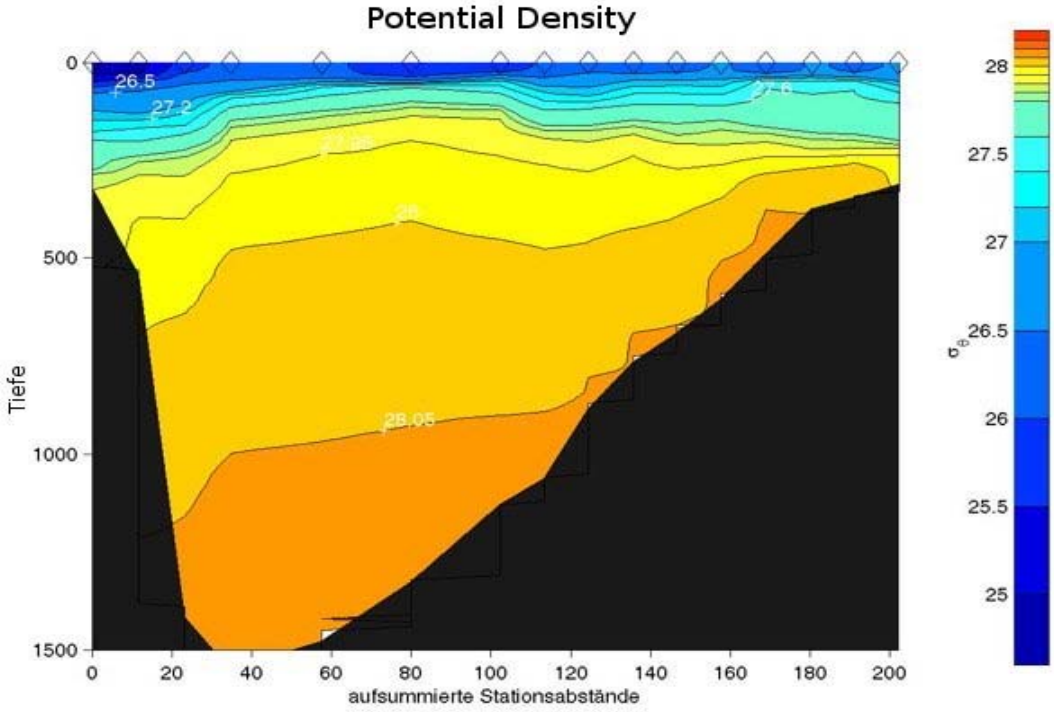

Figure 10: Distribution of Potential Density, section 2 (north of Denmark Strait)

The section at the sill indicates that the densest water is found in the deep channel at the Iceland side of the strait (Figure 7) and section 2 (Figure 10) also indicates that dense water is found at higher levels above the Iceland slope. The overflow water also comprises warmer, more saline and less dense water (Figures 5, 6, 7) that could derive from the Atlantic Water recirculating in Fram Strait.

To distinguish between these two sources TS-curves from the sill section (green), section 2 north of the sill (red), and from the floats in the Iceland Sea (blue) are plotted together (Figure 11). These curves indicate that the Iceland Sea water column is too cold and has too low salinity to significantly contribute to the overflow. The East Greenland Current water masses, however, are similar to these found at the sill, both in the densest part as well as in the warm and less dense layers above.

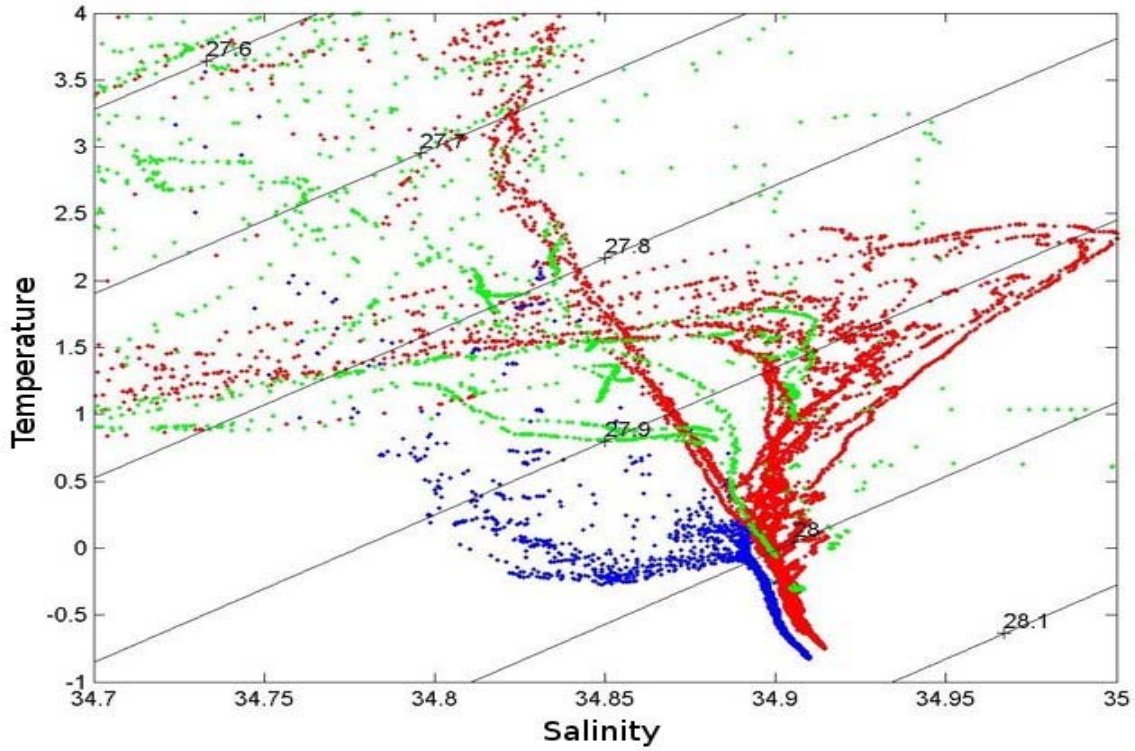

Figure 11: TS-diagram, blue: float data, green: section 1, red: section 2

This then suggests that the overflow, at least during the Discovery crossing mainly comes from the EGC. The densest part would then shift from the Greenland side to the Iceland side as the channel narrows and sill is approached. This is in agreement with the theory of channel flow crossing a ridge.

The water characteristics are determined from different data sets, the Discovery CTD data and the ARGO float, and there could be an error in sensor calibration, leading to the differences between the data. The area covered by the float tracks may not be representative for the part of the Iceland Sea that would contribute to the overflow. The float tracks suggest that the water recirculates in the Iceland Sea and, when leaving it rather moves towards the Norwegian Sea. The floats circulate at 1300m depth, which may not be representative for the water potentially contributing to the overflow. One way to remedy this would be to launch floats at the 300m level, which correspond to the density of the densest overflow water.

Seasonal Cycle of Water Mass Properties in the Iceland Sea
Observations and Mathematic Model

The Iceland Sea is a major source for Intermediate Waters in the Nordic Seas. These waters are formed through convection during winter and partly contribute to the overflow waters in Denmark Strait.

Since October 2005 continuous measurements of temperature and salinity profiles have been taken with ARGO profiling floats in the Iceland Sea. These autonomous floats drift at a depth of 1,000 m for a period of 10 days. They then sink to a depth of 1,300 m and ascent to the surface while measuring pressure, temperature and salinity at predetermined intervals (50 m steps from 1,300 m to 600 m, 25 m steps from 600 m to 500 m and 10 m steps from 500 m to the surface). At the surface the data and the GPS position of the float are transmitted via satellite to the ARGOS data centre. They then sink again to 1,000 m depth and the next drifting period starts. Figure 12 shows the surface positions of float No. 343.

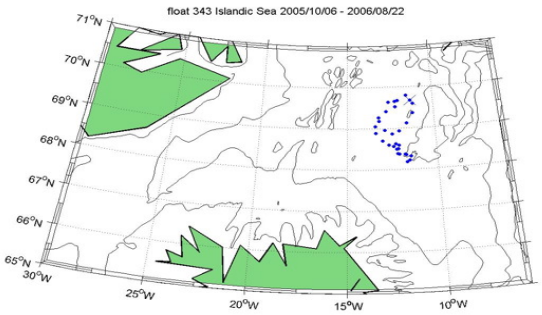

Figure 12: Positions of float 343 between 6. Oct. 2005 and 22. Aug. 2006

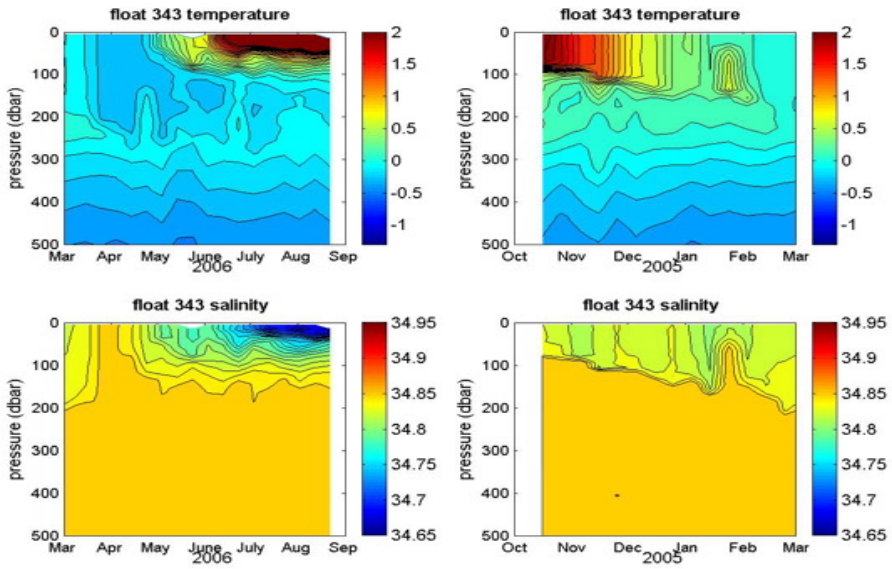

Figure 13: Seasonal Temperature and Salinity distributions from float data in '05 and '06

To illustrate the seasonal cycle of the stratification the development of temperature and salinity in the upper 500 m of the watercolumn are shown for the periods March to August and September to February (Figure 13). Solar radiation during the summer

months heats the upper layer with temperatures increasing from about –0.5° C to more than 8° C. A strong seasonal thermocline is formed. During the winter month with little solar radiation and stronger winds the upper layer cools and deepens through convection. During late winter the mixed layer reaches down to approximately 250 m to 300 m.

The applied model of heat transport in a vertical water column is given by the equilibrium of the time change of temperature and vertical eddy diffusion (equation 1), and by the flux of heat at the sea surface (equation 2).

$$\frac{\partial T}{\partial t} = \frac{\partial}{\partial z}\left(A(z) \cdot \frac{\partial T}{\partial z} \right) \qquad (1)$$

$$W = -A(z) \cdot \frac{\partial T}{\partial z}, z = 0 \qquad (2)$$

T = T(t, z) and A = A(z) denote time and depth dependent temperature and the coefficient of eddy heat diffusion, respectively. W(t) denotes the flux of temperature at the sea surface. This quantity is proportional to the heat flux. Having main features in view, this model is used for reproducing seasonal variations of temperature profiles as having been observed by floats in the Iceland Sea.

It is assumed that the heat flux is sinusoidal with a period of one year, taking the value zero in March. The value of the coefficient of eddy heat diffusion is prescribed as constant from the sea surface down to a depth of 200m, decaying from there exponentially to the exp(-2)th part of the upper mixed layer value at the sea bottom (500m). The differential equation (1) with boundary condition (2), representing time dependent forcing, is treated numerically. For this purpose the first order time derivative is replaced by a forward difference and the second order space derivative by a second order central difference. In (2) for the first order derivative a one sided difference is applied. The resulting time stepping procedure is performed using a time step Δt = 50 s and spatial grid point distance Δz = 10 m. Therefore, there are 50 depth levels at which the temperature is computed, and 630,720 time steps are needed to complete the cycle of a year. As cooling will lead to instabilities, convection must be considered in the model, too. This process is included into the model by a mixing mechanism having to be performed at the end of every time step.

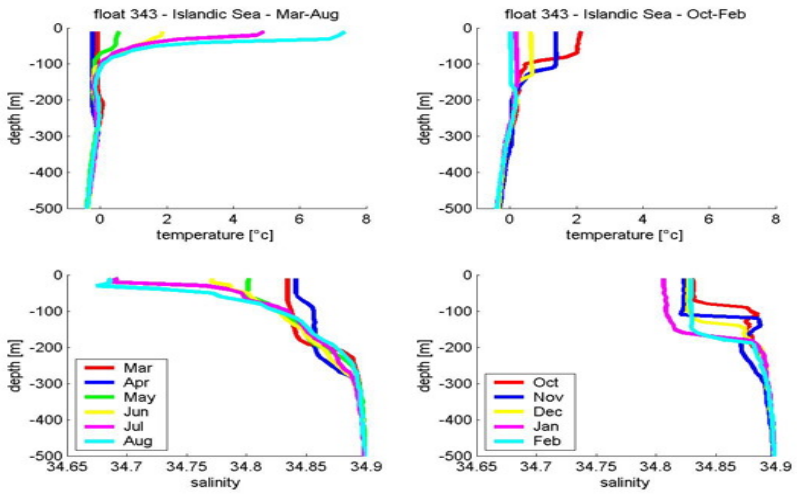

Figure 14: Temperature and Salinity profiles from float data

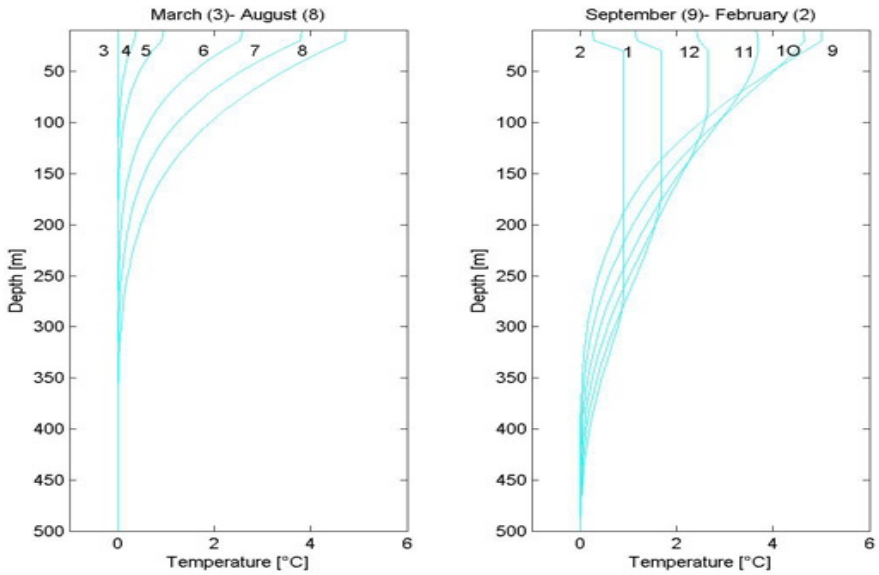

Figure 15: Seasonal Temperature profiles computed by the model

Figures 14 and 15 show the observed (14) and the computed (15) temperature profiles for the months March to August and for September to February, respectively. Although important processes have been neglected in this one-dimensional model, like advection, the profiles reflect some characteristic features of the observed profiles.

To these belongs the typically seasonally development of the temperature profile close to the surface. In summer a distinct warm water mixed layer appears with a strong vertical gradient at 100m depth, which, however, is weaker than in the observations (see Figure 14). This might be due to the coefficient of heat diffusion having been chosen too large in depths down to 200m. The surface temperature decay begins in September and properly reflects the observed one. The degradation of the stratification in winter and the typical deepening of the upper homogeneous layer is well reproduced by the model. This realistic deepening is brought about by the proper parameterisation of convection in the model.

It is straightforward to extend the model by also considering the change in time of salinity at the different depth levels. The numerical model for salinity only differs from that one for temperature by changing the dependent variable and by including salinity flux instead of W(t).

Moreover, values for the coefficient eddy salt diffusion may be chosen which differ from those used for eddy heat diffusion. Applying the convection mechanism in the combined temperature-salinity model requires computing the density by applying the equation of state at the end of every time step.

Freshwater Transport in the East Greenland Current

Global warming may cause dramatic climatic changes on earth. One change might be increasing freshwater entries in polar regions. A freshwater top layer would isolate the underlying warm water masses coming from the south. Due to this the North Atlantic Current (the northern offshoot of the Gulf Stream) would not cool down (become dense) and sink to the deep. This would weaken, and perhaps stop, the Atlantic Meridional Overturning Circulation (AMOC). Such changes may be detected by an increase in the freshwater transport in the East Greenland Current, which carries the freshwater from the Arctic Ocean and from Greenland ice melt to the North Atlantic. So it is always expedient to monitor the current freshwater transport in the Nordic Seas. We calculated the freshwater transport in the East Greenland Current, using data obtained on leg_2 of the RRS Discovery cruise D311.

Section 1, stations 43-48, 23.09.06-24.09.06

Station 43: 63°10,50' north
41°01,08' west

Station 48: 62°54,93' north
40°16,18' west

The measurements of temperature, salinity and depth recorded at the stations give us the thermo-haline structure of the East-Greenland Current on the shelf. We only considered the upper 200m .To find geostrophic velocities we use the dynamical method the specific volume anomalies and the geopotential anomalies. Before that we present the temperature, salinity and TS structure of the section (see Fig.16, 17, 18). Figure 16 shows that from the surface down to 160 m depth we have cold water up to station no. 46.

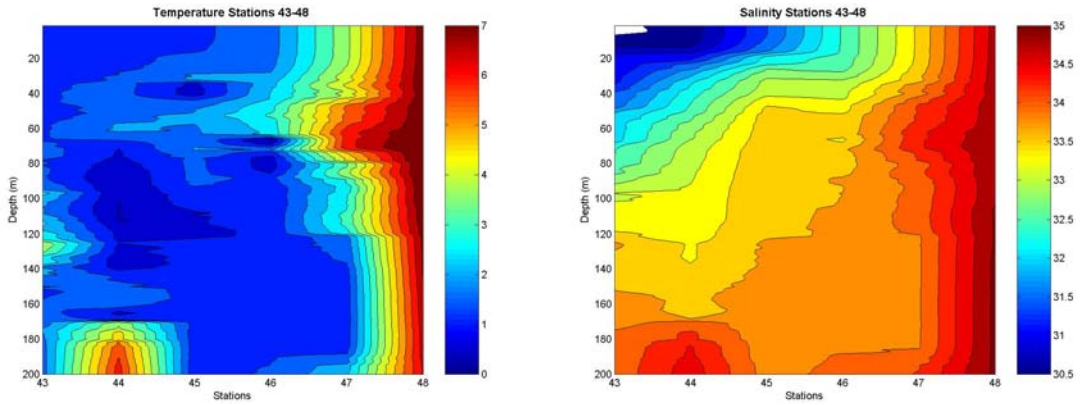

Figures 16 / 17: Temperature / Salinity distribution along the section

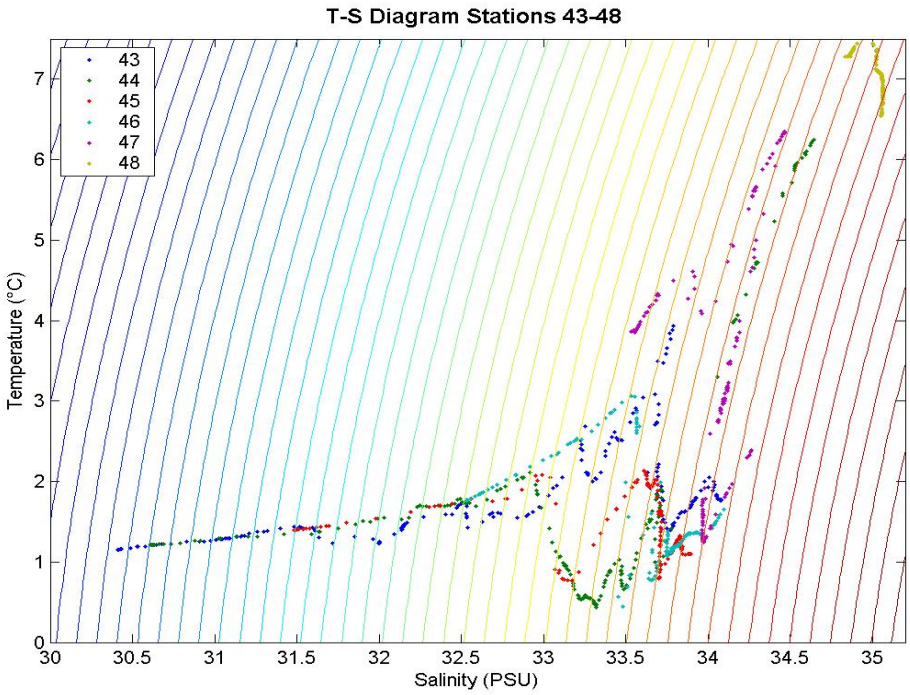

Figure 18: TS-diagram along the section

Looking at Figure 17 at this section we have low salinity between station 43-44. The interesting part can be localised in the upper region down to 90m from surface on. So we can concentrate on this zone of the East Greenland Current. In all three figures Atlantic Water and Polar Water can be clearly identified by their typical temperature, salinity and density values (Figure 19). To estimate the freshwater transport we have to determine the velocity of the current. Here we assume that the current is in geostrophic balance and that the velocity is zero at 200 meters. The barotropic part of the current is neglected.

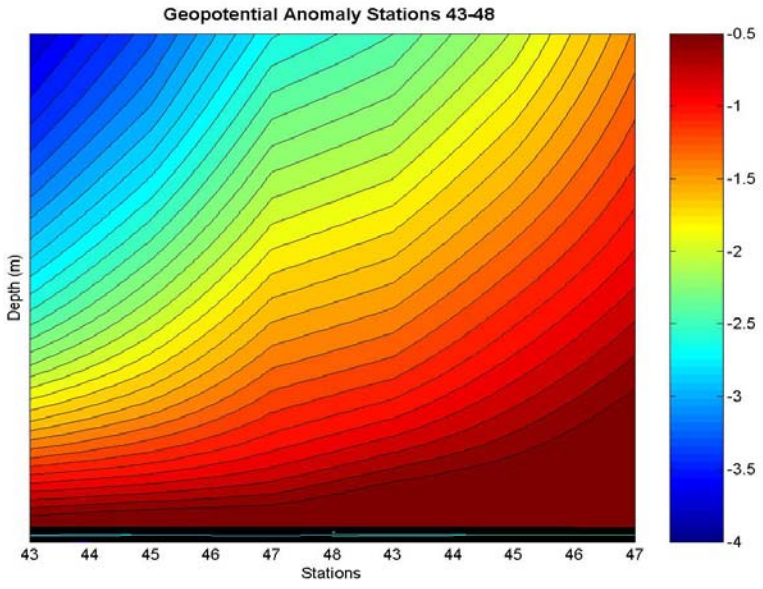

Figure 19: Geopotential Anomaly along the section

To discuss the geostrophic method we first introduce the concept of geopotential.
It is defined as the amount of work required to lift a mass M over a vertical distance dz against the force of gravity disregarding friction.

$$dw = M \cdot g \cdot dz$$

(g = 9,81 m/s^2, M: Mass, w : quantity, dz: vertical distance). So the geopotential (Φ) is defined by:

$$Md(\Phi) = dw = M \cdot g \cdot dz$$

It is given in joules/ kg or m^2/s^2. That means it represents potential energy changes per unit mass over a vertical section.

$$d(\Phi) = g \cdot dz = -(\alpha) \cdot dp$$

($(\alpha) = 1/(\rho)$). Integrating from ρ_1 to ρ_2 and writing $\alpha = \alpha_{35,\,0,\,p} + \delta\alpha$. We get:

$$- \Delta\,(\Phi)_{std} - \Delta\,(\Phi).$$

The first part is the standard geopotential equal on all stations. The second part gives us the geopotential anomaly (Figure 19) and is a function of S,T and p, given in dyn m; 1 dyn m = 10.0 J/kg. Use D for geopotential and using dynamical m, ($D_2 - D_1$) is close to ($z_2 - z_1$). The geopotential anomaly is first computed relative to the sea surface. To be conform with our assumption of no velocity at 200 m, the zero level has to be moved to this depth. This leads to a sea surface slope from Greenland towards the shelf break of about 20 cm over the section.

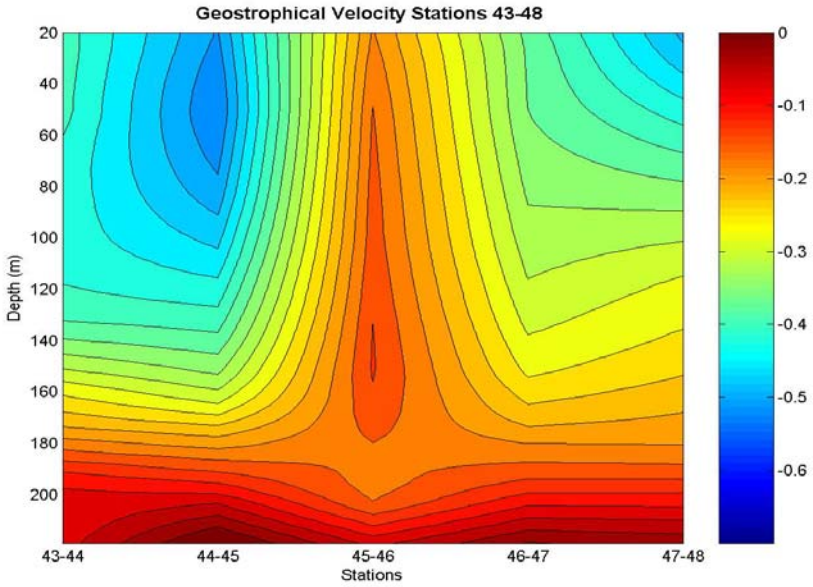

Figure 20: Geostrophical Velocity along the section

Figure 20 shows the geostrophical velocity. It shows, in combination with Figure 19, that we have a strong gradient between 120m and 140m depth, so we concentrate on this wedge. At 200m we have no geopotential anomaly, because in this depth the gradient of geopotential anomaly is set to zero.

In this phase we calculate the geostrophic velocity shear (V_1–V_2) between two levels 1 and 2 and the stations B and A.

$$(V_1 - V_2) = \frac{10}{L \cdot 2 \cdot \Omega \cdot \sin(\Phi)} \cdot (\Delta D_B - \Delta D_A)$$

We calculate the geostrophic velocity from the horizontal gradients in geopotential anomaly, recognising that it is relative to the surface.
Figure 20 shows the geostrophic velocity between stations 43 and 48. At the surface between stations 43 and 45 we can see, that the geostrophic velocity is higher than in the part of station 45 to 48. The geostrophic velocities show two high speed cores associated with low salinity there. One over the shelf break indicating another part of the East Greenland Current. We know that the water masses moves southwards but with different velocities. In this case we have to recognise that in geostrophic approximations the velocity at bottom has been set to zero (here at 200m depth). In reality we find a velocity at the bottom, so also friction. The freshwater transport T_{fresh} can be calculated as follows:

$$T_{fresh} = \sum_{j=1}^{m} \left(\sum_{j=1}^{n} 1 \cdot \frac{\Delta D_{(j+1)i} - \Delta D_{ji}}{f} \cdot \frac{35{,}2 - S_m}{35{,}2} \right)$$

(for S_m = mean salinity between j+1 and j). This formula includes all parts we calculated.

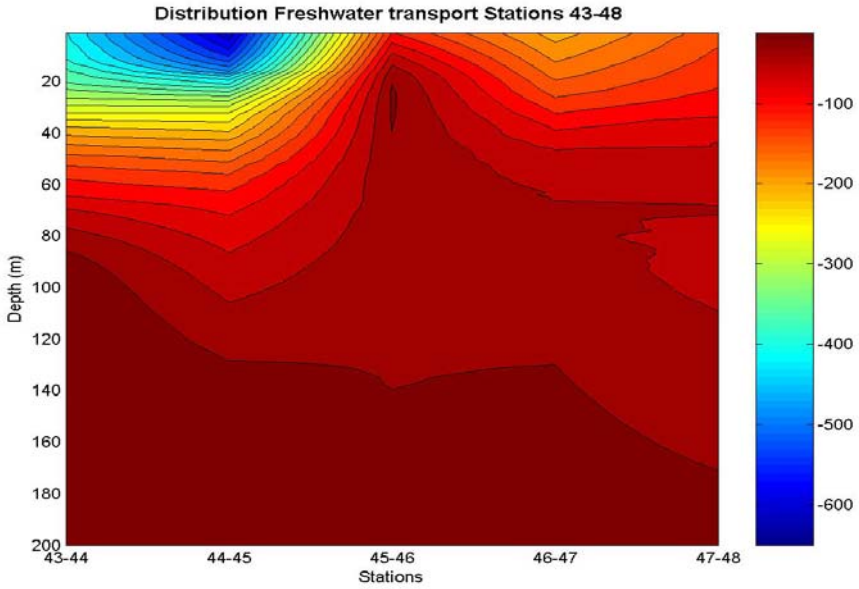

Figure 21: Freshwater distribution along the section

We also used the Coriolis parameter f (= 2 Ω sinϕ) which is f = 0,00013 1/s, for this latitude. The freshwater transport is given per 1 m layer in Sv (Sverdrup; = $10^6 m^3/s$), it is shown in Figure 21.The total transport of freshwater through the section is 0,06 Sv. We notice that freshwater transport is much more concentrated at the surface than at the bottom with a difference from 0 to 600 m^3/s. We can conclude that Polar freshwater, which is flowing southwards, mostly can be found in a wedge close to Greenland from surface down to 90 m depth on this section of the East Greenland Current, from here on the content of freshwater is decreasing rapidly.

Our result absolutely lies within the expected bounds, bearing in mind we only calculated the geostrophic part of the transport. Additionally we may hypothesise a contingent future evolution: In case of decreasing freshwater input, the stability of the stratification would decrease. From here on it would be easier that deep water masses mix with the surface layer and the thermohaline circulation would be unhinged. This would facilitate convection at high latitute and thus increase the strength of the thermohaline circulation. The salinity at the surface would get higher rates and we could recognise a faster convection. In case of increasing freshwater input we hypothesise that the convection may be reduced. The thermohaline circulation would then weaken, leading to a smaller transport of warm surface water towards the Nordic Seas and the Arctic Ocean. But this is only in the upper northern seas. To get more information about the freshwater transport in the East Greenland Current and its behaviour, different measurements are used. A good method of measuring the freshwater signal is using a combination of seacats and current meters.

Air Sea Heat Fluxes

During our cruise we measured the sea surface temperature every 30 second. The temperature ranged between 14.275°C and -0.99°C with a high variability on small scales. Generally there are three main reasons why the water temperature changes:

a) Advection
   Currents move different water masses with different temperatures and heat is transported horizontally.

b) Vertical mixing
   Vertical mixing between water layers can result in vertical heat transport.

c) Heat exchange with the atmosphere
   Latent and sensible heat fluxes between the water and the atmosphere and radiative fluxes change the upper ocean temperature.

The question we asked ourselves was to which degree the heat fluxes between the ocean and the atmosphere are responsible for changing the sea surface temperature.

The heat fluxes between ocean and atmosphere can be computed with bulk formulas, including the total irradiance (Q_{tir}), the latent and sensible heat flux (summed up as Q_{turb}), the longwave incoming radiation (Q_{lin}) and the longwave outgoing radiation (Q_{lout}).

$$Q_{heatflux} = Q_{tir} + Q_{turb} + Q_{lin} - Q_{lout}$$

The ship's instruments measured the position (latitude, longitude), the wind speed, the sea surface and the air temperature, the air pressure, the humidity and the total irradiance.
The latent and sensible heat flux was computed *as*:

$$Q_{turb} = \rho_a * c_h * c_p * u_a * (T_a - T_s)$$

ρ_a = density of air, c_h = heat transfer coefficient, c_p = specific heat of air, u_a = Wind speed, T_a= Air temperature, T_w = water temperature

The longwave incoming radiation has been computed as:

$$Q_{lin} = \varepsilon_a * \sigma * T_a^{\,4} \quad , \quad \varepsilon_a = 0.7829 * (1 + 0.2232 * Cl^{2,75})$$
$$= 0.7829 * (1 + 0.2232 * Cl^{2,75}) * \sigma * T_a^{\,4}$$

T_a = air temperature, $\sigma = 0.826 * 10^{-10}$, Cl = cloud coverage, ε_a= emissivity of the air

The cloud coverage was estimated by scientists and members of the ship crew; we compared two values here (60% and 75%).

The longwave outgoing radiation was computed using

$$Q_{lout} = \sigma * T_s^{\,4}$$

$\sigma = 0{,}826 * 10^{-10}$, T_s = water temperature

Finally the heat needed for the fluctuations of the sea temperature (Q_{sea}) was computed using

$$Q_{sea} = \rho_w * c_w * (\Delta T / \Delta t) * d$$

ρ_w = water density, c_w = specific heat of water, ΔT = temperature change, Δt = time period, d = upper water layer depth

The upper water layer depth was estimated to a value of 50 m. Furthermore we calculated a 1 hour mean for Q_{sea}. Figure 22 shows the total heat flux ($Q_{heatflux}$) with its single components.

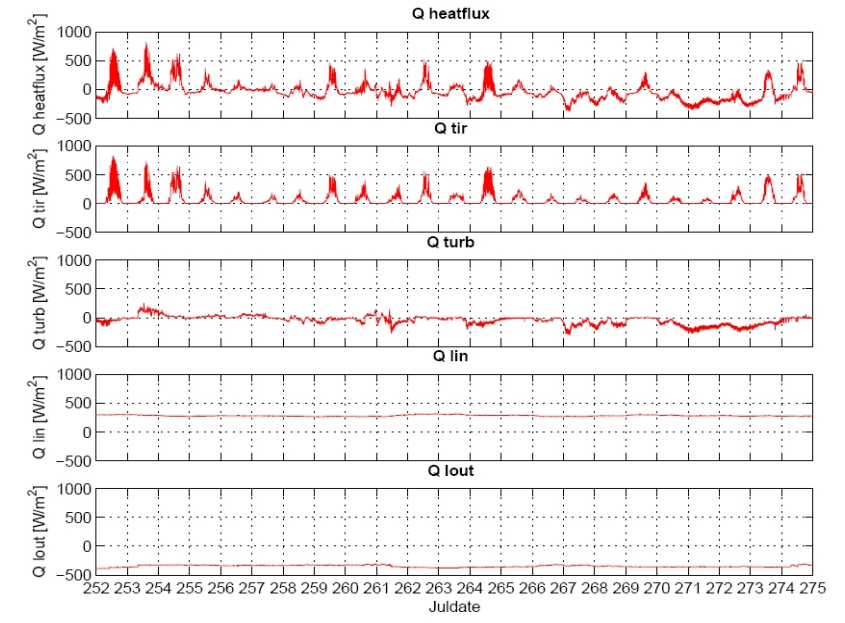

Figure 22: Heat Flux Q and its components

The heat flux has daily cycles, reaching from 820 W/m^2 to –387 W/m^2. This is mainly caused by the strong total irradiance during daytime and the longwave outgoing radiation during the night.

The daily mean heat flux, which we plotted in an additional graphic, shifts from INTO the ocean to INTO the atmosphere during the cruise. This agrees with a general shift from

the water-heating summer times to the water-cooling winter times. We were able to detect the change of these two periods, compare with Figure 23.

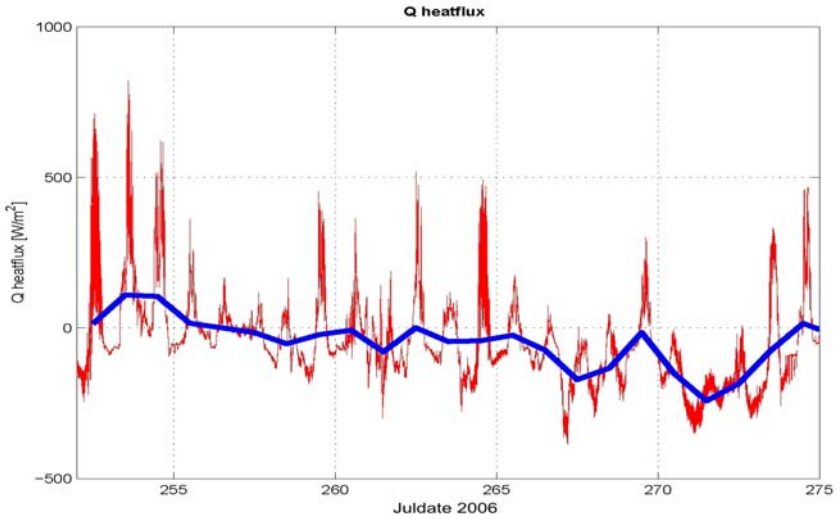

Figure 23: Heat Flux and its daily mean

We calculated the overall mean heat flux. It has a value of –46 W/m^2, which means a heat transfer from ocean to atmosphere. Figure 24 shows among other things the total air sea heat flux and the 1 hour mean for Q_{sea} during the whole cruise. On short time scales the air sea heat fluxes are not correlated with the heat fluxes needed to explain the ocean temperature change. The air sea heat fluxes fluctuate between –400 and 800 W/m^2, whereas the Q_{sea} values range between +/- 100 000 W/m^2. Therefore the air sea heat flux cannot be the main reason for the detected water temperature changes during our cruise.

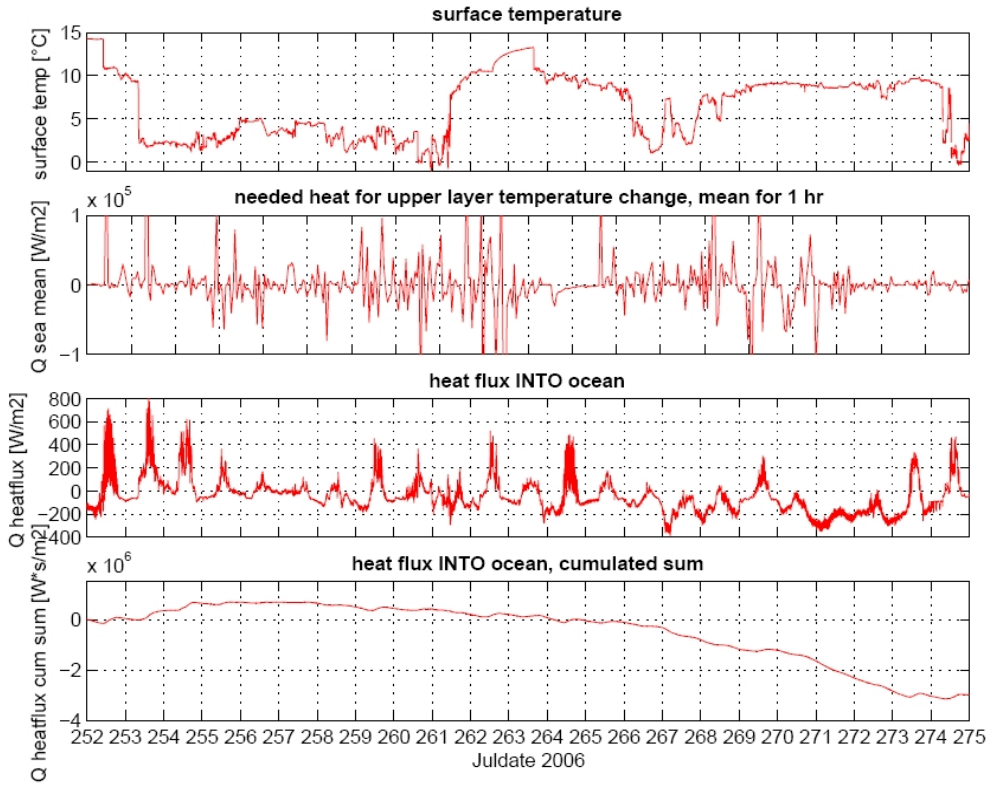

Figure 24: Surface Temperature, Q sea mean (1hr), Q heatflux, Q heatflux/cumulated sum

After Q_{sea} was compared with $Q_{heatflux}$ for the whole cruise, we concentrated on two other illustrative comparisons:

a. We checked the temperature delta (ΔT = 0.376°C) from a geographic position(67.0339 N, -24.7533 W) we crossed and measured two times within 5,67 days (255 16:44:00, 261 08:48:00). The motivation behind this was to be more secure that we measured the same water mass. The temperature increases by 0.376°C within this period, resulting in mean Q_{sea} of 158 W/m^2. This is supposed to be caused by strong incoming radiation, however the heat flux was in the opposite direction and cannot explain the heating of the water, see Figure 25. We assumed the heat fluxes kept the same, even though we did not hold our position.

b. Furthermore, we compared the $Q_{heatflux}$ and Q_{sea} of a short time period of 6 hours. (Figure 26). During the chosen time slot, from day 263 00:00:00 to 06:00:00, the sea surface temperature slowly increased from 12.643°C to 12.931°C, which results in a Q_{sea} of 1000 to 4000 W/m^2. But within the same period a negative heat flux, in line with a heat transfer into the atmosphere, was computed. The values are about 75 to 120 W/m^2. That shows that neither the amount of heat flux nor its direction can explain the temperature decrease.

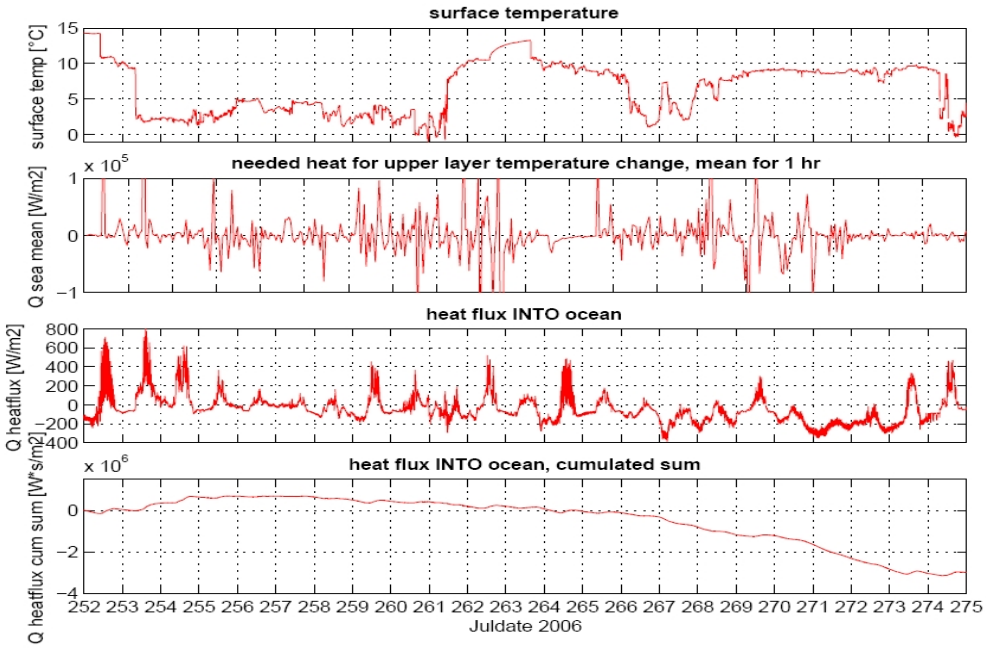

Figure 25: Q heatflux, Q heatflux/cumulative sum for a choosen geographic position (67.0339N, -24.7533W) we crossed twice

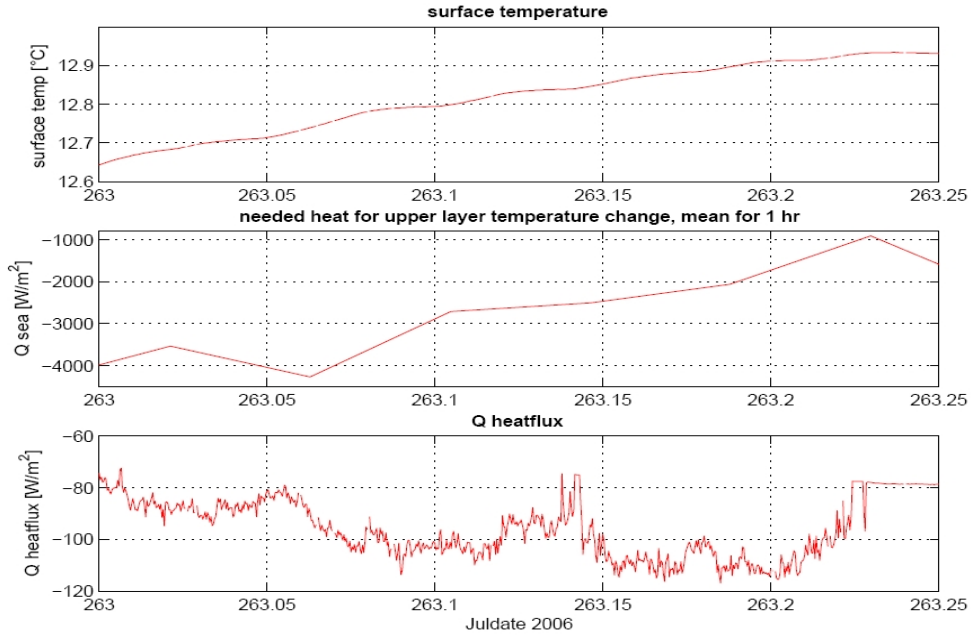

Figure 26: Surface temperature, Q sea mean (1hr), Q heatflux during the chosen time period from day 263 00:00:00 to 06:00:00

Our work on the total heat fluxes certainly shows the transition from summer to winter. The curve of the daily mean falls from the positive into the negative domain. Also, the overall mean heat flux with a value of –46 W/m^2 shows the negative heat balance, characteristically for this season and latitudes.
Nevertheless, we have a few uncertainties in our estimations, that are in particular the cloud coverage and the upper water layer depth that we needed for computing Q_{sea}.
There was no measurement of the cloud covering, that's why two calculations with 60% and 75% mean covering where done as a comparison. The resulting mean heat fluxes are –33 and –46 W/m^2, a difference of more than 40%.
Another estimation was done with the depth of the upper water layer. The needed heat for the measured temperature change strongly depends on the estimated water layer depth. We took a depth of 50 m for our computing, which seems to be reasonable. Further work on CTD data could probably improve this estimation.
During our cruise the vessel was located in different water regimes with different sea surface temperatures caused by ocean currents. It is sure that advection of other water masses plays a huge part in heat transport in this area. That is also one reason why we could not find a correspondence between the heat fluxes and the sea surface temperature.
Finally there could be heat transport by vertical mixing between water layers, which we also left out of consideration.

Interpolation methods for hydrographic sections across a sloping bottom

The aim of cruise D311 in the Irminger Sea was to measure transports and mixing in the overflow through Denmark Strait. One method to estimate volume, heat and freshwater transports of the overflow is to use hydrographic sections across the dense plume south of Denmark Strait. CTD measurements provide a good vertical resolution. However, since they are time-consuming, the sections usually consist of only few vertical profiles leading to low horizontal resolution. When transports are calculated, the stations need to be interpolated across the section. The overflow plume runs along the Greenland shelf

slope, thus profiles at different depths are taken. The common horizontal interpolation of these profiles is problematic at the bottom where the overflow water is situated.

The aim of this project is to apply two alternative interpolation methods for hydrographic sections across a sloping bottom. This may improve the calculation of heat and freshwater transports. An improved interpolation could then be used to find the minimum number of profiles in a section needed to estimate transports within a given error range.

The following interpolation methods are applied to the standard hydrographic section ASOF 3 recorded in 2005. This section is situated 500 km downstream of the Denmark Strait sill and consists of 15 stations spaced over 175 km. As an example interpolations are carried out for the temperature field.

The common horizontal method interpolates the temperature field along isobars (Figure 27). The results are reasonable for surface and intermediate layers. In the bottom layer, parts of the temperature field are missing that cannot be interpolated due to different profile depths. These are the triangles that are formed by the intersection of real bottom (red line) and the bars corresponding to each station. The step-like structure of the bottom is also found in the interpolated temperature field close to the bottom where the isotherms are strongly inclined. The overflow plume is not described realistically with the interpolation along isobars.

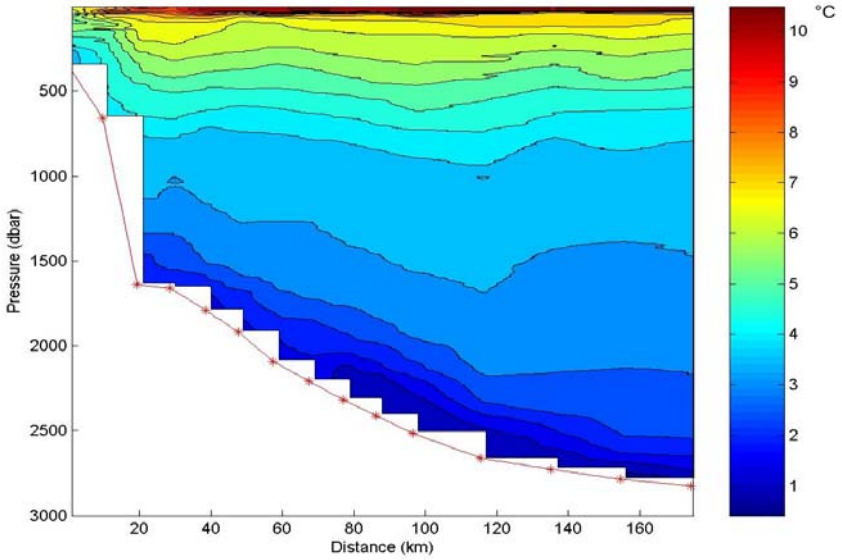

Figure 27: Temperature field from interpolation along isobars (red line indicates the bottom)

The interpolation of the bottom layer can be improved by taking the bottom pressure of each station as reference level (Figure 28). With this transformation, the isotherms close to the bottom are nearly horizontal. A horizontal interpolation now produces appropriate results for the temperature distribution in the overflow plume. Finally, the temperature field is transformed back to the isobaric levels (Figure 29). However, the step-like structure appearing in the bottom layer using the common interpolation is now shifted to the surface. The lower part of the resulting temperature distribution can be used to calculate the heat transport of the overflow plume.

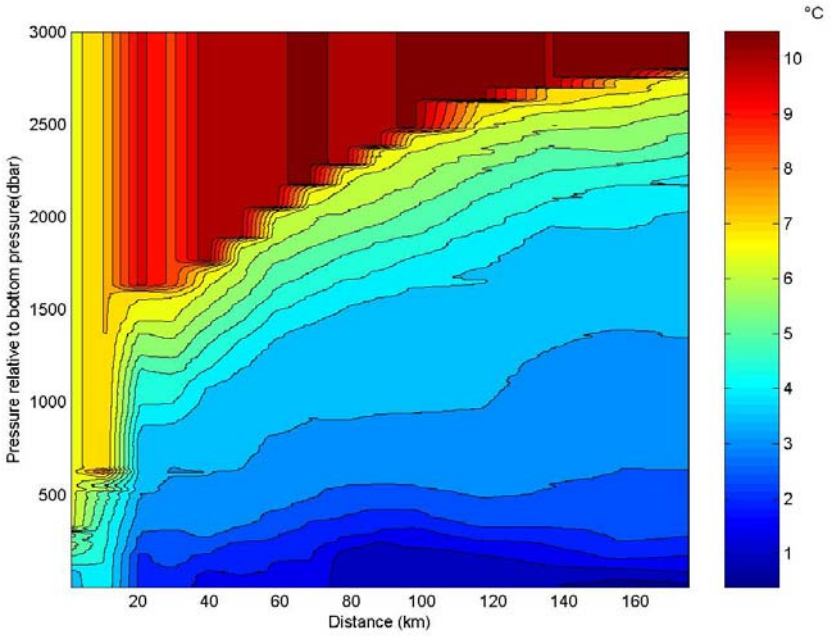

Figure 28: Bottom Pressure as reference level

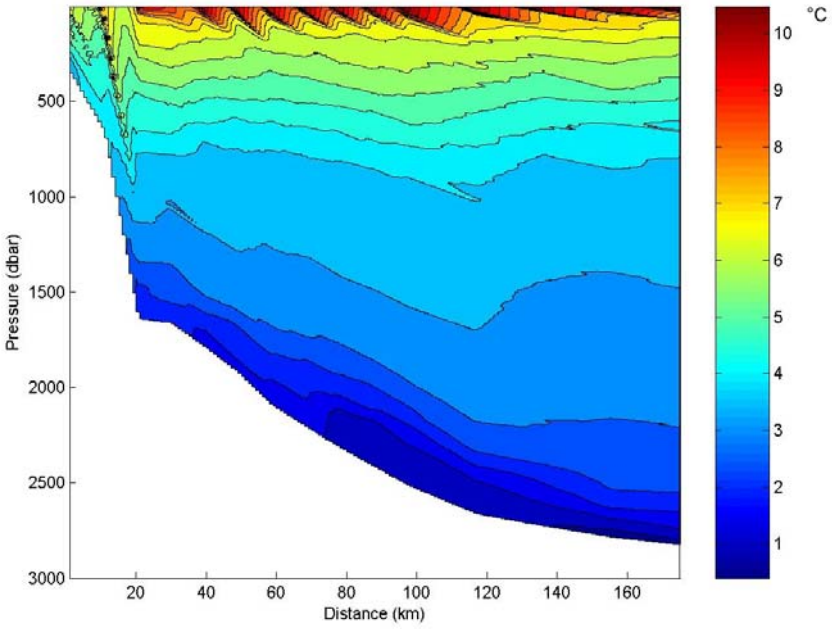

Figure 29: Interpolation with the Bottom Pressure as reference level

When the heat transport of the whole section is to be computed, an appropriate temperature field can be obtained combining the resulting upper layer of the first and the lower layer of the second method. However, this mixture of methods may cause problems at the interface.

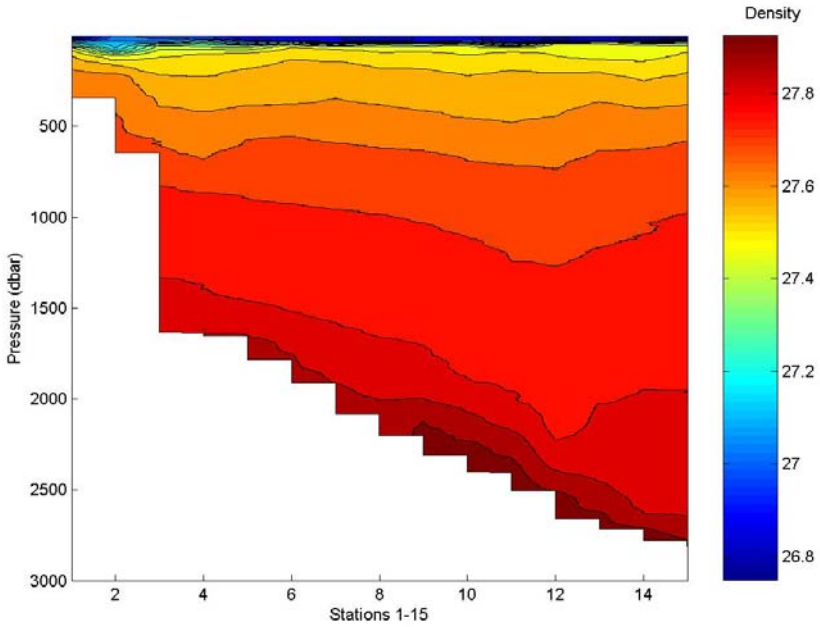

Figure 30: Density distribution

The density distribution of the section (Figure 30) suggests another approach would be to interpolate along lines of constant density. This can be accomplished by a transformation of the temperature profiles from pressure into density space. This transformation, the interpolation in density space and the back transformation are described below.

The dependence of density on pressure determines the transformation. As the density values in the profiles are not monotonically increasing, they are sorted to increase with increasing pressure. This makes sense physically as we do not expect instabilities. The temperature values are sorted simultaneously with the same index. To establish a unique transformation between density and pressure coordinates, density values are rounded to 10^{-4} kg/m^3 and the temperatures corresponding to constant density values are averaged. The temperature profile for each station is interpolated to a density grid with a spacing of 10^{-4} kg/m^3. The temperature field is interpolated horizontally, i.e. along the isopycnals (Figure 31). The interpolated temperature field in density space is transformed back to pressure space by averaging over 1dbar bins (Figure 32).

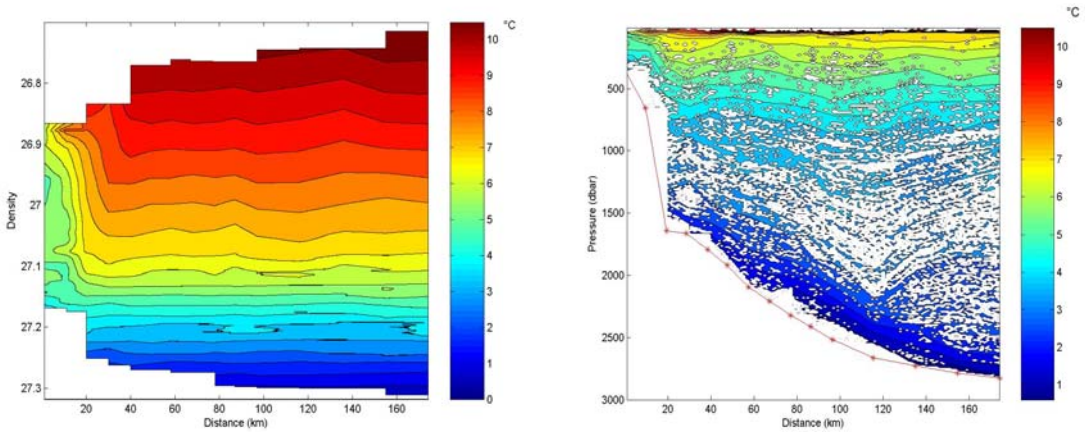

Figures 31 / 32: Interpolation along isopycnals

In the areas where density changes only little within a large pressure range, the back transformation to a 1dbar grid causes a loss of temperature values. These can be seen as empty values in the temperature distribution shown in Figure 32. However, as this happens in regions of small gradients, the missing values can be linearly interpolated. Figure 33 shows the final result.
The interpolation along isopycnals does not produce a step-like structure in the overflow plume. It fails where isopycnals intersect the bottom or the surface. In density space (Figure 31), this corresponds to the step problem for different bottom depths in pressure space.

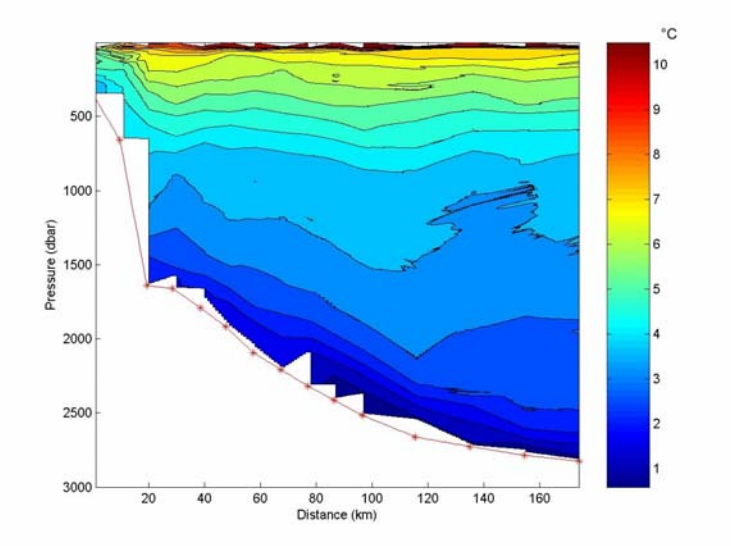

Figure 33: Vertically interpolated temperature field from interpolation along isopycnals

The interpolation relative to the bottom pressure and along isopycnals are both an improvement compared to the interpolation along isobars where the bottom layer is concerned. The two methods adapt the structure of the sloping isopycnals in the bottom layer. However, we do not know which of the three interpolation methods presented here closest resembles the real fields as they differ from each other (Figure 34). A next step would thus be to create an idealised data set to determine their accuracy. Heat and freshwater transports from interpolated temperature and salinity fields could then be compared to the known overall transport.

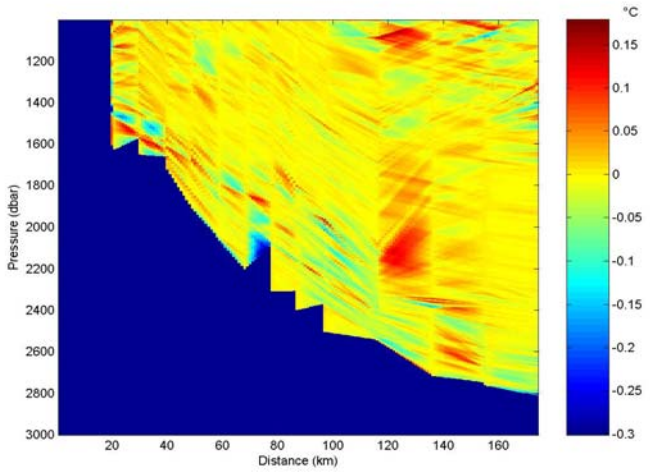

Figure 34: Difference between the temperature fields from interpolation with a flat bottom and interpolation along isopycnals for depths below 1000m

Meso-scale Eddies in the Denmark Strait Overflow plume
Data analysis of the UK1-05 mooring

Moorings are one particular fixed point method for measuring the Denmark Strait Overflow plume in the northern Atlantic. On September 23rd, 2006, during our cruise D311 we recovered the mooring UK1-05 at position 63° 29' N 36° 18' W, which had been deployed in August 2005. During this 13.5 month period three Seabird SBE 37 (microcats) measured continously conductivity and temperature at three different depth (top: 1595dBar = 1574m, middle: 1773dBar = 1748m, bottom: 1962dBar = 1933m). The two upper microcats also measured pressure.

The idea for this study was to identify meso-scale cold core eddies in the Denmark Strait Overflow plume by analysing the variability in the data set provided.
The theories that explain observed meso-scale eddies in the Denmark Strait Overflow is based on the physical mechanisms of vortex stretching and baroclinic instability. Eddies are formed as the dense water descends the slope from the sill (Figure 35). To conserve the potential vorticity of the water column while stretching it starts to spin cyclonically. The thickness in the dense water layer increases below the eddies and adopts a domelike structure.

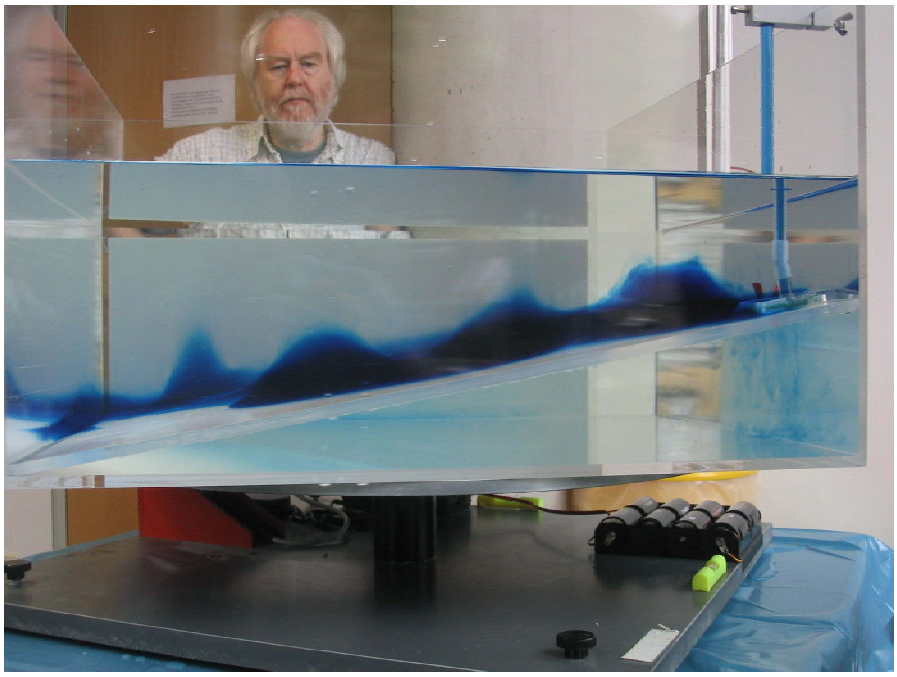

Figure 35: Tankexperiment – Dome shaped eddies

We expected to recognize the cold core eddies in our salinity, temperature and density signals.

The original data set consists of conductivity, temperature and pressure values taken every 10 over the whole period of 13.5 months. By examining the pressure data from the upper two instruments we realized that the mooring slid down the slope about ten meters after the first 38 days.

We calculated the bottom instrument's pressure by using its estimated depth and the variability from the upper levels, and included the change after 38 days (Figure 36). The high frequency variability in the pressure data is probably caused by the tides and internal waves.

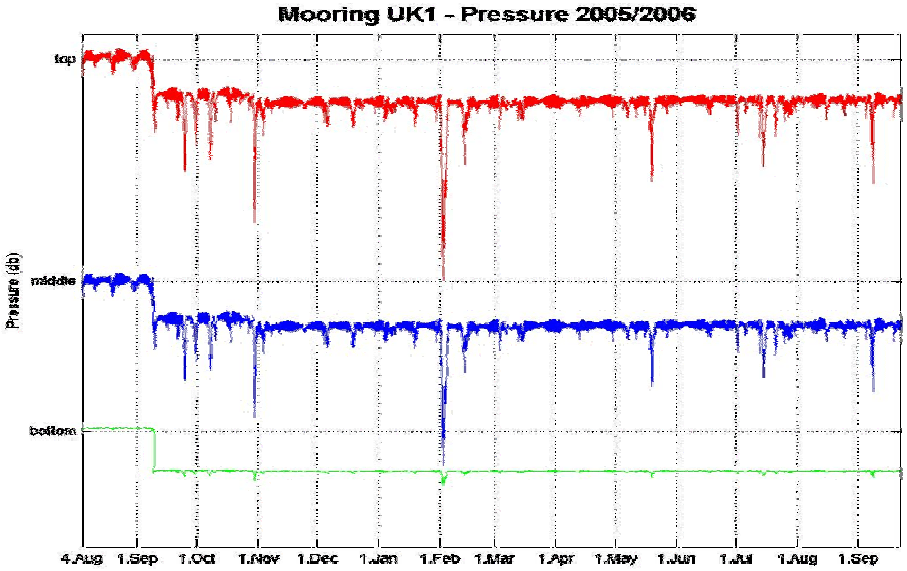

Figure 36: Mooring UK1 – Pressure 2005/2006

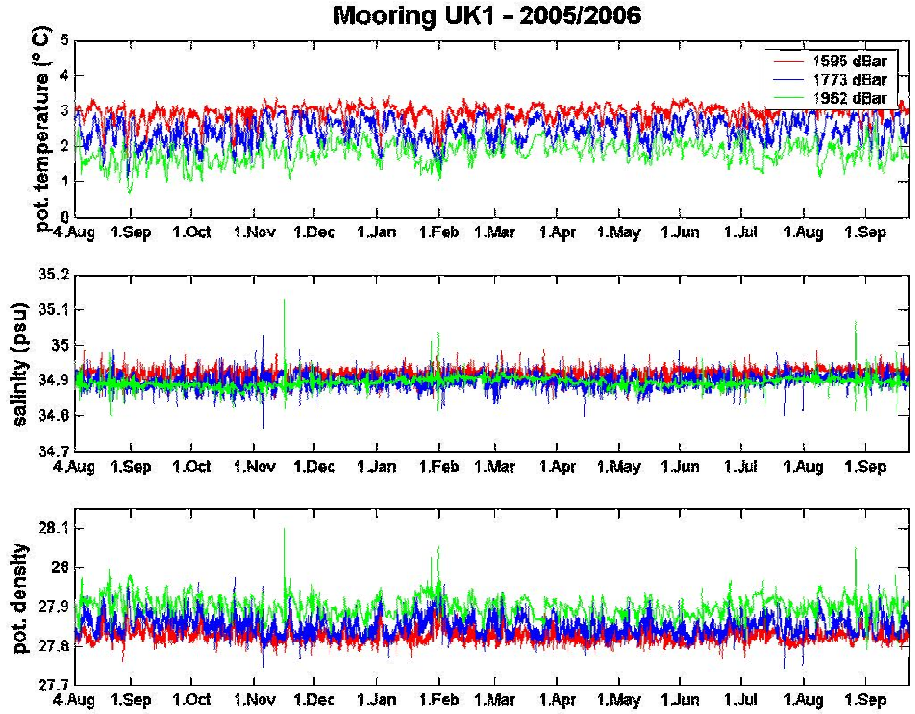

Figure 37: Mooring UK1 – pot. Temperature, Salinity, pot. Density

The large peaks (Oct, Nov, Feb, May, Jul, Sep) might be caused by higher current velocities knocking down the instruments. The vertical movement of the instruments shown by the pressure data also influences the temperature and conductivity values.

The next step was to compute salinity, potential temperature and potential density. To get a first impression of the variability range we created time plots of these parameters (Figure 37). The mean potential densities are 27.8249 $\pm$ 0.0153 (top), 27.8526 $\pm$ 0.0230 (middle) and 27.9022 $\pm$ 0.0230 (bottom).

Figure 37 shows the expected strong high frequency variability in the data. When we compare these time series with Figure 36, we find a peak consistency with pressure peak values in all parameters (e.g. November and February).

The spectrum of the pressure signal given by discrete Fourier transformation of the top data (Figure 38) appears to confirm this suggestion. Figure 38 shows three peaks, the SM1 tide, the M2 tide and the inertial period. For 63° 29' N the inertial period is 13.341 h. To extract the timescales of interest we used a bandpass filter. The filter cuts off the frequencies below 1/(15 days) and higher than 1/(36h). Figure 39 shows an example of the effect of the filter on the bottom salinity spectrum, while Figure 40 shows the unfiltered and the filtered data as time-series.

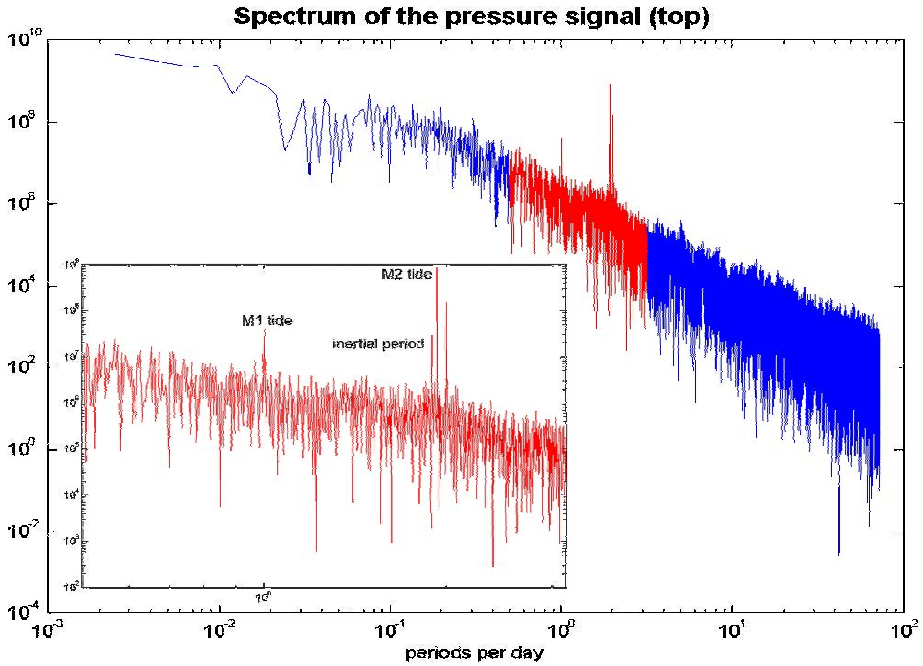

Figure 38: Mooring UK1 – Pressure 2005/2006

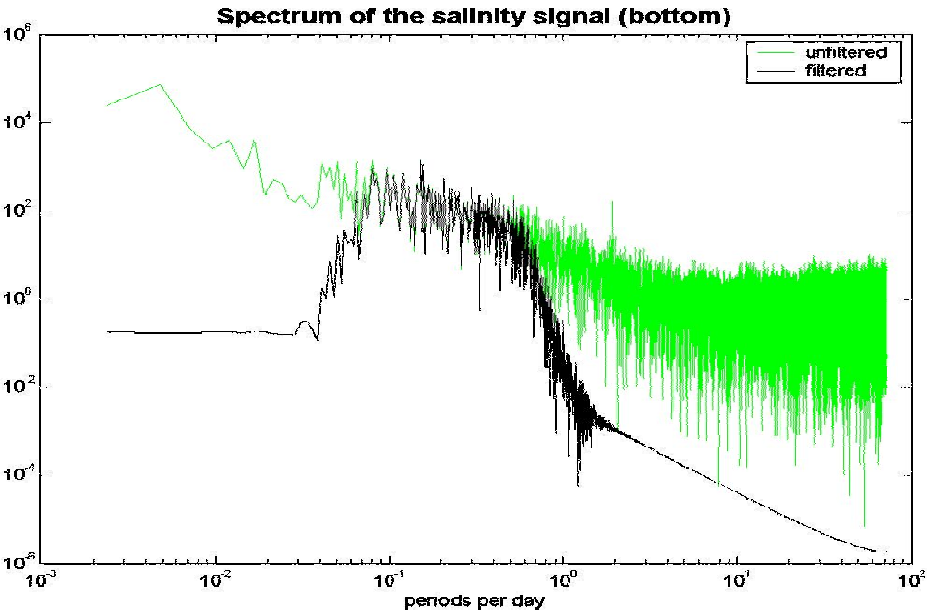

Figure 39: Spectrum of the salinity (bottom)

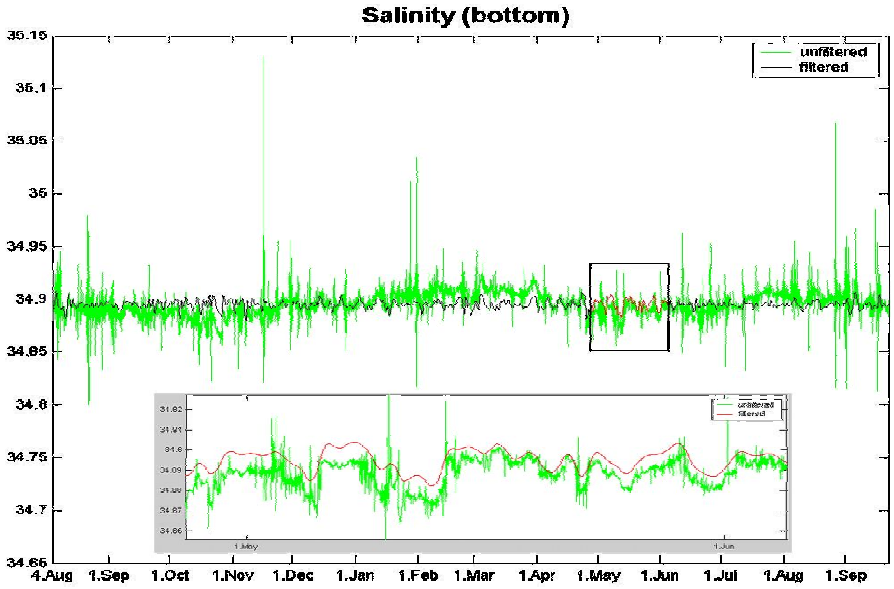

Figure 40: Salinity (bottom) – filtered, unfiltered

Then each parameter (potential temperature, salinity and potential density) was interpolated between the three depths in steps of 10 dBar. The filtering of our data made it possible to pick out every 18th value (three hour steps) without losing the signals of our interest. Afterwards we created contour plots for each parameter for the period of two months (Figures 41(a, b, c)). We added the 27.85 isopycnal to each plot, which can be used to define an upper boundary for the overflow plume. In these contour plots, particularly in potential temperature, we can now identify about 3-4 cold core eddies per months in the Denmark Strait Overflow plume. The mean depth of the plume upper boundary is 1,710 m with a standard deviation of 60 m.

Finally we compared our results with CTD measurements at the position of UK1-05 from 1998 to 2003. We created a pressure/potential density plot from these CTD data and added three lines at the depths of the UK1-05 microcats and the mean potential densities plus standard deviations of the mooring measurements (Figure 42a). The CTD data sets of the different years show a high variability. Some data sets do not even fit in the range of the mooring mean data's standard deviations. So they can hardly be used for identifying cold core eddies.
Then we picked a single potential density value at the three UK1-05 depths out of each CTD data set and interpolated between these three. The result is shown in figure 41b. It gives an impression of the differences between original data (Figure 42a) and interpolated data (Figure 42b). There is a great loss of vertical spatial resolution by using only 3 depths points.
For both, vertical spatial and temporal high resolution of the measurements we suggest to deploy Jojo-moorings, which measure continuously in small depth and time intervals.

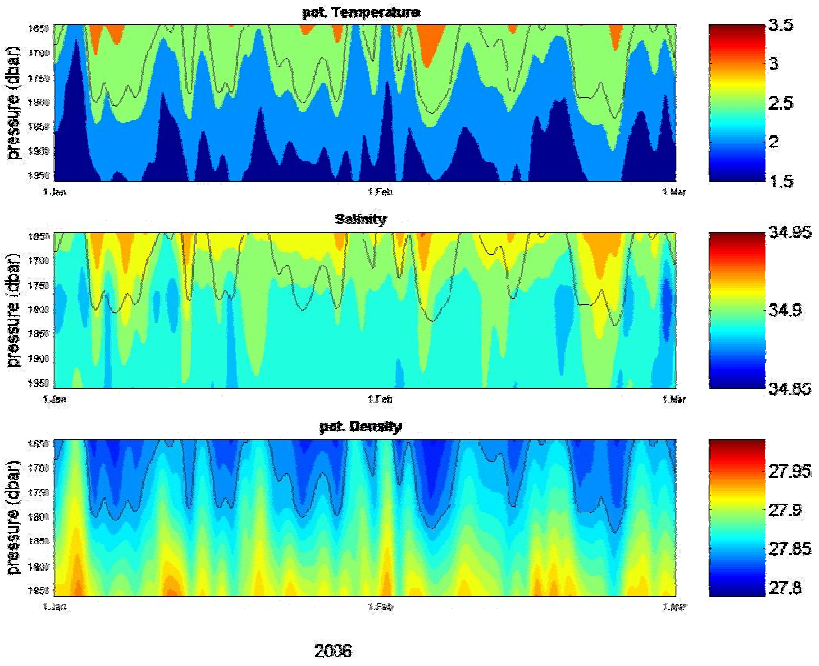

Figures 41(a, b, c): Contour plots - Pot. Temperature, Salinity, Pot. Density

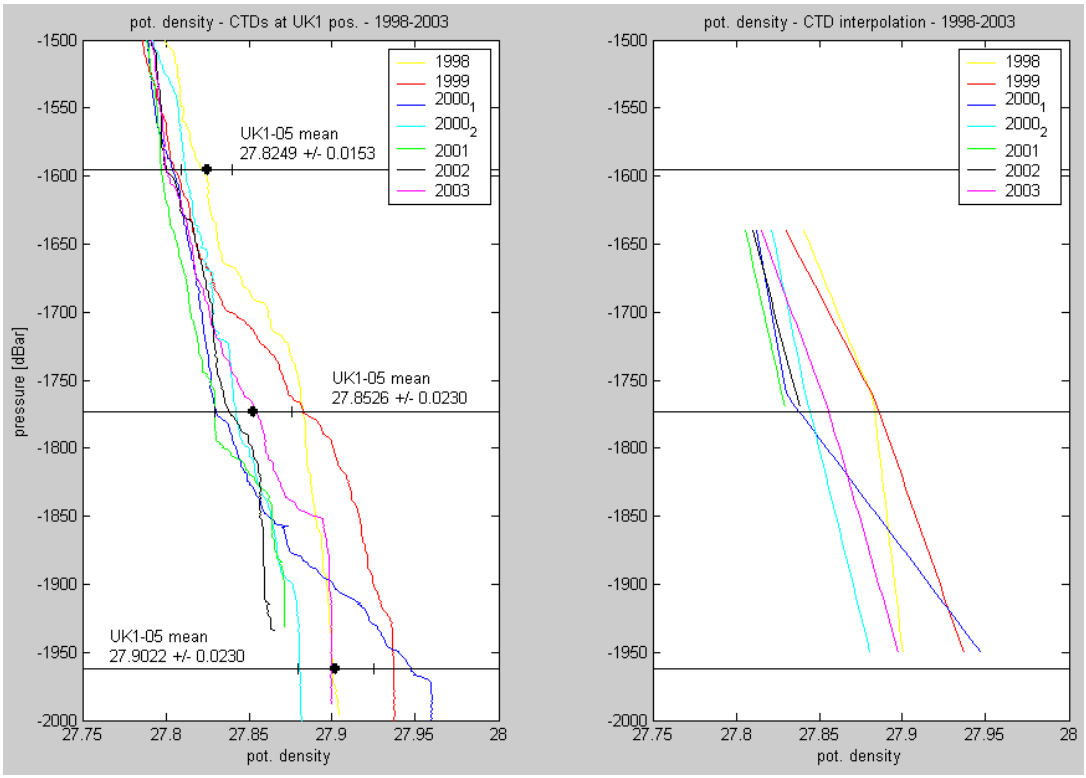

Figure 42 (a, b): CTD data at UK1 Position 1998-2003

7. Acknowledgements

We like to thank Captain Peter Sarjeant, his officers and crew of RRS DISCOVERY and the UKORS technical staff for their support of our measurement programme and for creating a very friendly atmosphere on board.

Financial support by the different funding agencies of the participating scientific groups is gratefully acknowledged.

Mooring recoveries:

DS-ADCP:	V425-04	66° 07.24’ N	27° 16.19’ W		580 m
		Released:	10.09.2006	13:50 Z	
		Not Recovered			
ASOF:	G2-05	63° 07.19’ N	35° 32.50’ W		2545 m
		Released:	22.09.2006	07:50 Z	
		Not Recovered			
ASOF:	UK2-05	63° 16.94’ N	35° 52.24’ W		2320 m
		Released:	22.09.2006	10:29 Z	
		On deck:		11:30 Z	
ASOF:	G1-05	63° 21.99’ N	36° 04.20’ W		2160 m
		Released:	22.09.2006	12:22 Z	
		On deck:		13:20 Z	
ASOF:	UK1-05	63° 29.07’ N	36° 18.10’ W		1954 m
		Released:	22.09.2006	14:29 Z	
		On deck:		15:37 Z	
ASOF:	F1/2-05	63° 35.48’ N	36° 38.90’ W		1687 m
		Released:	22.09.2006	16:52 Z	
		On deck:		17:42 Z	
ASOF:	ADCP-21	63° 00.27’ N	40° 31.49’ W		219 m
		Grappled:	23.09.2006	08:38 Z	
		On deck:		10:41 Z	
ASOF:	TUBE-21	63° 00.27’ N	40° 32.75’ W		295 m
		Released:	23.09.2006	12:38 Z	
		Not Recovered			

Mooring deployments

ASOF:	TUBE-28	63° 00.22’ N	40° 32.73’ W		305 m
		Top Buoy in water:	23.09.2006	14:35 Z	
		Anchor released:		15:22 Z	
ASOF:	ADCP-28	63° 00.88’ N	40° 31.22’ W		218 m
		Anchor at bottom:	25.09.2006	11:35 Z	
		63° 01.05’ N	40° 30.95’ W		205 m
		ADCP at bottom:	25.09.06	12:16 Z	
ASOF:	F1/2-06	63° 35.44’ N	36° 39.26’ W		1717 m
		Top Buoy in water:	26.09.2006	09:23 Z	
		Anchor released:		10:22 Z	
ASOF:	UK1-06	63° 29.01’ N	36° 17.98’ W		1988 m
		Top Buoy in water:	26.09.2006	13:15 Z	
		Anchor released:		13:49 Z	
ASOF:	G1-06	63° 22.10’ N	36° 04.36’ W		2158 m
		Top Buoy in water:	26.09.2006	15:43 Z	
		Anchor released:		16:13 Z	

ASOF:	UK2-06	63° 16.92’ N	35° 52.09’ W	2358 m
		Top Buoy in water:	26.09.2006	17:37 Z
		Anchor released:		18:06 Z

CTD stations

Stat.	Cast	Date	Time	Position		Bottom
No.	No.	mmddyy	UTC	Latitude	Longitude	depth
001	001	090906	1518	64 30.87 N	23 21.31 W	146
002	001	091006	0926	66 00.28 N	26 44.19 W	380
002	002	091006	1100	66 00.01 N	26 44.70 W	368
003	001	091006	1539	66 07.30 N	27 17.75 W	565
004	001	091006	1944	66 01.20 N	26 51.43 W	516
005	001	091006	2147	66 03.06 N	26 57.42 W	618
006	002	091106	0344	66 03.94 N	27 04.11 W	669
007	001	091106	0612	66 05.41 N	27 11.20 W	645
008	001	091106	0911	66 09.03 N	27 22.59 W	505
009	001	091106	1054	66 10.58 N	27 29.06 W	500
010	001	091106	1325	66 12.29 N	27 35.68 W	501
011	001	091106	1534	66 16.25 N	27 50.66 W	470
012	001	091106	1831	66 19.55 N	28 06.16 W	350
013	001	091106	2122	66 23.86 N	28 21.25 W	338
014	001	091106	2345	66 28.10 N	28 34.66 W	331
015	001	091206	0140	66 32.42 N	28 50.95 W	316
016	001	091206	0332	66 36.54 N	29 05.34 W	323
017	001	091206	2154	67 09.95 N	22 40.28 W	309
018	001	091306	0007	67 15.97 N	22 40.03 W	342
019	001	091306	0206	67 21.65 N	22 40.62 W	642
020	001	091606	1533	67 28.10 N	22 39.50 W	512
021	001	091606	1713	67 33.94 N	22 39.68 W	580
022	001	091606	1932	67 39.91 N	22 40.71 W	666
023	001	091606	2126	67 46.06 N	22 41.01 W	NaN
024	001	091606	2353	67 52.19 N	22 40.19 W	857
025	001	091706	0204	67 58.02 N	22 39.34 W	1070
026	001	091706	0437	68 03.92 N	22 39.75 W	1015
027	001	091706	0725	68 16.15 N	22 40.28 W	1300
028	001	091706	1009	68 28.32 N	22 41.11 W	1422
029	001	091706	1313	68 35.62 N	23 06.96 W	1527
030	001	091706	1601	68 39.64 N	23 19.68 W	1415
031	001	091706	1812	68 43.87 N	23 32.69 W	532
032	001	091706	2029	68 48.16 N	23 45.87 W	321
033	001	091906	0915	64 39.9 N	23 14.2 W	NaN
034	001	092106	1600	63 22.4 N	31 27.3 W	NaN
035	001	092206	0712	63 07.0 N	35 33.1 W	2545
036	001	092206	1026	63 16.7 N	35 52.5 W	2320
037	001	092206	1220	63 21.7 N	35 03.8 W	2160
038	001	092206	1425	63 28.7 N	36 17.9 W	1954
039	001	092206	1649	63 35.2 N	36 38.7 W	1687
040	001	092306	0735	63 01.0 N	40 31.8 W	219
041	001	092306	1102	63 00.4 N	40 32.2 W	295
042	001	092306	1433	63 00.78 N	40 31.32 W	223
043	001	092306	1730	63 10.0 N	41 01.19 W	233
044	001	092306	1849	63 06.96 N	40 52.25 W	290
045	001	092306	2102	63 04.00 N	40 43.60 W	270
046	001	092306	2245	63 00.62 N	40 34.50 W	328

047	001	092406	0036	62 57.86 N	40 25.81 W	240
048	001	092406	0244	62 54.74 N	40 16.42 W	1297
049	001	092506	1135	63 00.86 N	40 31.23 W	218
050	001	092506	1538	63 01.70 N	39 57.96 W	1540
051	001	092606	1022	63 35.48 N	36 17.97 W	1717
052	001	092606	1349	63 28.09 N	36 17.97 W	1982
053	001	092606	1612	63 22.10 N	36 04.36 W	2160
054	001	092606	1805	63 16.91 N	35 52.09 W	NaN
055	001	092606	2301	63 01.87 N	35 28.99 W	2650
056	001	092706	0806	63 10.15 N	35 44.34 W	2498
058	001	092906	1854	65 29.98 N	31 10.09 W	375
059	001	092906	2118	65 25.13 N	31 06.09 W	660
060	001	092906	2345	65 20.22 N	31 01.51 W	970
061	001	093006	0202	65 15.37 N	30 54.92 W	1210
062	001	093006	0406	65 10.23 N	30 50.60 W	1499
063	001	093006	0636	65 05.10 N	30 45.69 W	1757
064	001	093006	0911	65 00.12 N	30 40.90 W	1892
065	001	093006	1214	64 55.32 N	30 35.63 W	2030
066	001	093006	1506	64 50.48 N	30 30.20 W	2138
067	001	093006	2022	65 00.71 N	29 15.18 W	1452
068	001	093006	2233	65 05.14 N	29 20.15 W	1711
069	001	100106	1654	65 10.20 N	29 25.05 W	1654
070	001	100106	0231	65 15.16 N	29 30.11 W	1521
071	001	100106	0424	65 20.02 N	29 34.74 W	1338
072	001	100106	0632	65 24.68 N	29 39.79 W	1065
073	001	100106	0828	65 29.83 N	29 46.34 W	658
074	001	100106	1003	65 35.15 N	29 50.34 W	344
075	001	100106	1353	65 58.02 N	28 50.23 W	406
076	001	100106	1454	65 54.76 N	28 45.23 W	477
077	001	100106	1556	65 51.01 N	28 40.70 W	539
078	001	100106	1713	65 48.90 N	28 36.44 W	674
079	001	100106	1928	65 46.11 N	28 29.93 W	829
080	001	100106	2200	65 43.44 N	28 24.48 W	920
081	001	100206	0051	65 40.36 N	28 19.73 W	1005
082	001	100206	0331	65 32.23 N	28 15.56 W	896
083	001	100206	1824	66 10.49 N	27 28.94 W	893
084	001	100206	1854	66 10.20 N	27 28.21 W	904
085	001	100206	2032	66 06.08 N	27 10.19 W	495
086	001	100206	2303	66 02.53 N	26 55.00 W	631
087	001	100206	0122	65 59.06 N	27 21.96 W	586
088	001	100306	0341	65 54.76 N	27 48.98 W	654
089	001	100306	0541	65 51.90 N	28 12.78 W	629
090	001	100306	0734	65 46.82 N	28 32.12 W	624
091	001	100306	0955	65 41.72 N	28 56.07 W	917
092	001	100306	1215	65 31.69 N	29 15.33 W	1051
093	001	100306	1354	65 35.75 N	29 22.35 W	773
094	001	100306	1555	65 28.08 N	29 06.36 W	1250
095	001	100306	1827	65 24.08 N	29 39.74 W	1099
096	001	100306	2055	65 15.14 N	29 58.98 W	1378
097	001	100406	0108	65 10.15 N	30 28.62 W	1510
098	001	100406	0350	65 06.99 N	30 55.73 W	1620
099	001	100406	0857	65 27.51 N	32 18.27 W	816
100	001	100406	1050	65 22.85 N	32 18.63 W	1179
101	001	100406	1249	65 16.73 N	32 12.21 W	1435
102	001	100406	1529	65 06.75 N	32 03.54 W	1784

Institut für Meereskunde
der Universität Hamburg
Bundesstr. 53
20146 Hamburg
Germany

Technical Reports

1-84 Baudner, H., K. Jancke and D. Quadfasel: CTD-data obtained in the Red Sea during 21-30 May 1983, RV SAGAR KANYA.

1-85 Meincke, J. and E. Mittelstaedt: Forschungsschiff METEOR, Reise Nr. 69 NORDOSTATLANTIK 84, NOAMP III. Berichte der wissenschaftlichen Leiter.

2-85 Verch, N. and D. Quadfasel: Hydrographic observations in the Norwegian Trench during 23 March - 17 April 1983, VALDIVIA cruise 10.

3-85 Backhaus, J., J. Bartsch, D. Quadfasel and J. Guddal: Atlas of monthly surface fields of air pressure, wind stress and wind stress curl over the North Eastern Atlantic Ocean for the period 1955-1982.

1-86 Hainbucher, D., J. Backhaus and T. Pohlmann: Atlas of climatological and actual seasonal circulation patterns in the North Sea and adjacent shelf regions: 1969-1981.

2-86 Quadfasel, D. and M. Ungewiß: Large-scale hydrographic structure of the upper layers in Fram Strait during the Marginal Ice Zone Experiment, 1984.

3-86 Quadfasel, D., E. Schelenz and N. Winkel: Marginal Ice Zone Experiment 1984. CTD-data obtained from RV VALDIVIA.

1-87 Quadfasel, D. and N. Verch: Seasonal variability of temperature in the Red Sea: XBT-sections from MCS "UBENA" in 1985 and 1986.

2-87 Quadfasel, D. and D. Grawunder: NORDMEER 86 - RV VALDIVIA cruise 48. CTD-observations in the Greenland Sea.

3-87 Verch, N., D. Quadfasel and S. Selchow: Hydrographic observations in the Tyrrhenian Sea during 26.2-25.3.1986. RV SONNE cruise 41 (HYMAS).

4-87 Boehlich, M. and J. Backhaus: Atlas simulierter Strömungen in der südwestlichen Ostsee für sommerliche Bedingungen.

1-88 Schauer, U.: VALDIVIA-Fahrt Nr. 61 (25.07.-23.08.1987)

2-88 Quadfasel, D.: VALDIVIA Reise 67 (1.2.-26.2.1988) Grönlandsee

3-88 Backhaus, J., J. Bartsch, P. Damm, D. Hainbucher, T. Pohlmann, D. Quadfasel and G. Wegner: Hydrographische Bedingungen und Zirkulation in der Nordsee im Winter und Frühjahr 1987/88 - Eine physikalische Hintergrundstudie zur extremen Planktonblüte im Frühjahr 1988.

4-88 Radach, G., J. Berg, B. Heinemann and T. Zachmann: Berichte über die Arbeiten des Teilprojektes P4 "Mathematische Modelle von Energie- und Stofftransporten durch die unteren tropischen Stufen des pelagischen Ökosystems der Nordsee.

5-88 Quadfasel, D., and M. Ungewiß: MIZEX 87 - RV VALDIVIA cruise 54. CTD observations in the Greenland Sea.

6-88 Backhaus, J.: On the circulation around the Faroe Islands and the adjacent continental slope: Experiments with a three-dimensional barotropic model.

1-89 Verch, N., M. Ungewiß, K. Schulze and D. Quadfasel: MINDIK - RV METEOR cruise 5. CTD observations in the Red Sea and Gulf of Aden.

2-89 Verch, N., M. Petzold, P. Mahnke and D. Quadfasel: Hydrographic bottle data obtained in the Red Sea and Gulf of Aden during RV METEOR cruise 5 - MINDIK 1987.

3-89 Schönfeld, W., B. Heinemann, G. Radach and P. Damm: Die ECOMOD - Datenbank, ein Hilfsmittel mariner Ökosystem-Forschung. Datenbericht 1988.

4-89 Meincke, J., and D. Quadfasel: "VALDIVIA"-Reise 78 - Grönlandsee. Fahrtbericht.

5-89 Ambar, I., J. Backhaus, A. Fiuza, P. Mahnke and D. Quadfasel: Hydrographic observations in the Tejo-estuary during September 1985.

6-89 Damm, P.: Klimatologischer Atlas des Salzgehaltes, der Temperatur und der Dichte in der Nordsee, 1968 - 1985.

7-89 Schauer, U.: VALDIVIA - Reise 86. Arktisfront. 9.8.89 - 5.9.89 Bodø-Hamburg. Fahrtbericht.

8-89 Quadfasel, D.: "Valdivia" Reise 87, Faroe-Shetland Kanal, 14.-24. September 1989, Fahrtbericht.

9-89 Latarius, K. and G. Gerdts: VALDIVIA cruise 72, 1.-22. July 1988. CTD observations in the North Sea and Irish Sea.

1-90 Frische, A. and D. Quadfasel: SULU SEA RV SONNE Cruise 58. Hydrographic observations in the South China Sea and Sulu Sea.

2-90 Moll, A. and G. Radach: Wärme- und Strahlungsflüsse an der Grenzfläche Wasser-Luft berechnet bei Feuerschiff FS ELBE 1 in der Deutschen Bucht: 1962-1986.

3-90 Bohle-Carbonell, M., P. Damm and A. Frische: VALDIVIA Reise 92. Deutsche Bucht - Skagerrak, 12. Februar - 2. März 1990.

4-90 Quadfasel, D. and B. Rudels: Some new observational evidence for salt induced convection in the Greenland Sea.

5-90 Quadfasel, D.: "Valdivia" Reise 104, Islandsee, 15.-31. Oktober 1990, Fahrtbericht.

6-90 Moll, A. and G. Radach: ZISCH Parameter Report. Compilation of measurements from two interdisciplinary STAR-shaped surveys in the North Sea (Vol. I: Graphic Reports).

7-90 Moll, A. and G. Radach: ZISCH Parameter Report. Compilation of measurements from two interdisciplinary STAR-shaped surveys in the North Sea (Vol. II: Data Lists).

8-90 Hähnel, M.: VALDIVIA Reise 100, Arktisfront, 17. Juli bis 18. August 1990, Fahrtbericht.

1-91 Hähnel, M. and F. Schirmer: ADCP-Workshop 1991 in Hamburg, Vortragszusammenfassungen.

1-92 Latarius, K.: Current measurements in the Greenland Sea and West Spitsbergen Current obtained with satellite-tracked drifters during spring 1987 to summer 1989.

2-92 Dippner, J.: Mesoscale variability of the German Bight - an atlas of circulation, sea surface density and sea surface heights.

1-93 Quadfasel, D.: Valdivia Reise 131, Hamburg-Aberdeen-Stornoway-Bodø, 11. Januar-25. Februar 1993, Fahrtbericht.

1-94 Quadfasel, D.: Valdivia Reise 141, Hamburg-Tromsoe-Tromsoe-Hamburg, 7. Februar - 1. April 1994, Fahrtbericht.

2-94 Rudels, B., H. Friedrich and K. Schulze: Valdivia Reise 136, 15. Mai - 17. Juni 1993, Grönlandsee, Fahrtbericht.

1-95 Vajen, T., K. Herklotz, H. Haak and J. Bock: Ozeanographisches Seminar Wintersemester 1994/95. Hydrographie und Zirkulation der südostasiatischen Gewässer. Literaturstudie über den Indo-Pazifischen Einstrom.

1-96 Quadfasel, D.: Cruise Report, VALDIVIA cruise V160, TASC'n TEACH, 5.-16. July 1996, Hamburg - Torshavn - Reykjavik.

1-97 Quadfasel, D.: Cruise Report, VALDIVIA cruise V164, TASC'n TEACH II, 12.-21. May 1997, Hamburg - Torshavn.

2-97 Quadfasel, D.: Cruise Report, VALDIVIA cruise V165, ESOP II - ACSYS, 21. May - 9. June 1997, Torshavn - Longyearbyen.

3-97 Moll, A.: ECOHAM1 User Guide - The Ecological North Sea Model, Hamburg, Version 1.

4-97 Backhaus, J.: Fahrtbericht VALDIVIA Reise V167. ACSYS, ARKTIEF, SFB 313, ESOP II. Longyearbyen – Hamburg, 2. Juli – 27. Juli 1997.

5-97 Quadfasel, D., J. Meincke, J. Backhaus, Th. Knutz, M. Koch und B. Dümcke: Arbeits- und Erfahrungs-bericht über den Einsatz von drei verankerten Autonomen Profilierenden Geräteträgern im Projekt ACSYS vor Spitzbergen im Sommer 1997.

1-98 Quadfasel, D.: Cruise Report, SONNE cruise SO127 BENGALWOCE, Port Klang – Malé, 17 December 1997 – 7 January 1998.

2-98 Quadfasel, D.: Cruise Report, VALDIVIA cruise V171, ACSYS, Teach and SFB 512, Hamburg - Torshavn – Reykjavik, 15. June – 2. July 1998.

3-98 Hainbucher, D., Wei Hao: Cruise Report, DONG FANG HONG 2 cruise 01, AMBOS - AMREB, Qingdao – Qingdao, 23. September 1998 – 8. October 1998.

1-99 Karstensen, J.: The extended OMP analysis, An analysis package for MATLAB, Version 1, Hamburg.

2-99 Moll, A. und L. Ehlers: Zeitschriften-Verzeichnis, Institut für Meereskunde, März 1999.

3-99 Hainbucher, D., Wei Hao: Cruise Report, DONG FANG HONG 2 cruise 02, AMBOS/AMREB, Qingdao – Qingdao, 27. April 1998 – 12.May 1999.

1-00 Backhaus J.O., Hegseth E.N., Wehde H., Hatten K., Logemann K., Nedderhut H., Arndt C.: Cruise Report: Phyto - Convection, VALDIVIA cruise 176, Hamburg - Thorshavn, 26.Feb - 20.Mar 1999, VALDIVIA cruise 178, Tørshavn - Reykjavik, 08.Apr - 26.Apr 1999.

1-00 Hainbucher, D.,: Cruise Report, POSEIDON cruise POS 264, Tørshavn 25. August - 10. September 2000.

1-01 Mintrop, L.: Cruise Report, Winter in the Northeast Atlantic, POSEIDON cruise 267, Kiel – Madeira, Jan. 13-29.,2001

2-01 Hainbucher, D.: Cruise Report, S/V KOMMANDOR JACK cruises 02 & 03, Torshavn-Torshavn-Leith, 12. July – 29. July 2001

2-02 Hainbucher, D. and C. Mertens: Cruise Report, POSEIDON cruise 294, Reykjavik – Torshavn – Torshavn – Kiel, 06.09.2002 – 01.10.2002

1-03 Hainbucher, D. and A. Rubino: Cruise Report, POSEIDON cruise 298/2, Brindisi – Palermo, 12.05.2003 – 28.05.20031-04

2-03 Hainbucher, D.: Cruise Report, POSEIDON cruise 303, Reykjavik - Torshavn - Galway, 11. 09. – 23.09. – 24.09. – 06.10.2003

1-04 Quadfasel, D.: Cruise Report FS Alexander von Humboldt 44-04-12 Rostock - Reykjavik – Galway – Kiel 7.8. – 12.8. – 31.8. – 5.9.2004

2-04 Quadfasel, D.: Cruise report RRS Charles Darwin CD164/164b Reykjavik – Glasgow, 23. September – 12. October 2004.

1-06 Quadfasel, D.: Cruise report RRS Discovery D311 Reykjavik - Reykjavik - Reykjavik, 8. September – 20.September – 6. October 2006.